Post Access Report

Assessing cost-effective spatially distributed current measurements from microFloat swarms for tidal energy resource characterization and model validation

Awardee: Applied Physics Laboratory – University of Washington

Awardee point of contact: Trevor Harrison

Facility: Pacific Northwest National Laboratory

Facility point of contact: Zhaoqing Yang

Date: October 13, 2023

TEAMER
Testing & Expertise for Marine Energy

EXECUTIVE SUMMARY

This project evaluated how high-resolution, spatially distributed field data can be used to refine and validate site-scale hydrodynamic simulations of tidal channels. Use of such spatially-distributed field observations or site-scale hydrodynamic simulations will be needed for producing accurate predictions of tidal energy production over larger arrays of tidal turbines.

Here, we compared field observations from a series of short surveys in Agate Pass taken on August 20th, 2020 against a high-resolution hydrodynamic model of the site. The field observations included water velocities measured by station-keeping ADCP measurements, drifting downward-looking ADCPs, and microFloats, gathered by researchers at APL-UW under a previous project.

Supported by this TEAMER funding, PNNL refined an existing hydrodynamic model of Puget Sound, WA, to produce a high-resolution (10-20 m horizontal, 1 m vertical) subdomain model of Agate Pass, and conducted model simulations over the field survey periods at 30 second intervals. Using these high-resolution maps of tidal currents, APL-UW and PNNL compared the model against the field observations.

Results indicated agreement between the model and the field observations, with a few notable trends:

- PNNL performed subdomain model refinement to improve model accuracy. While there was overall improvement, the improvement in error statistics is not significant when comparing to NOAA fixed-station ADCP data.
- Comparison of model and microFloat data showed moderate overall agreement, though larger than comparisons between the model and NOAA fixed-station ADCP data.
- There is better agreement between model and field observations during ebb surveys than during flood. This is likely due to the location of the field observations relative to spatially constrained vs. unconstrained flow. During ebb surveys, observations were primarily restricted to the channel. During flood, the observations extended from within the channel into the body of Port Orchard, primarily carried by a jet. While the model captures the presence of the jet, the exact location is unlikely to match reality, resulting in differences between model and observations.
- Comparisons between simulated microFloat trajectories and the observed ones also confirmed the model bias in simulating flow fields in Agate Pass. The model-data difference is consistent with previous comparisons between NOAA fixed-station ADCP measurements and the model.

The microFloat has the potential to provide cost-effective, spatially-distributed resource assessments in tidal, river, and ocean energy applications. Through the model-data analysis pursued here, we sought to determine how microFloat data products may be best utilized in model validation, improving their TRL and aiding in current-energy site-characterization. The answer was, while somewhat unsatisfying but not surprisingly, “It’s complicated.” The methodology implemented here is straightforward and can be applied to future model-observation comparisons, but the field data set was too sparse (i.e., too few and too short deployments) to draw broadly applicable conclusions. To further the investigation, a bigger field observation data set would be needed, preferably multiple sequential tidal cycles (a few days) gathered over a minimum of two different periods of the lunar cycle. The microFloat data can be used to support model validation for tidal energy resource characterization and assessment.

1 INTRODUCTION TO THE PROJECT

Tidal energy resource characterization typically occurs in two phases: regional-scale site assessment and local-scale site characterization. Regional-scale assessments rely on high resolution hydrodynamic model simulations that are validated against one or more stationary Acoustic Doppler Current Profilers (ADCP). This inherently limits validation to the location with ADCP data and resource assessments of adjacent waters have implicit uncertainty. Thus, for local-scale characterization, IEC technical specifications recommend deployment of an ADCP at the planned location of a turbine, a method which has been feasible for projects to date in which only a small number of turbines have been deployed. As larger arrays are pursued, placing an ADCP at each turbine location is unlikely to be cost-effective or practically feasible. Thus, system-scale site characterizations will necessitate spatially comprehensive (horizontal and vertical) field data, either for direct reference or for validation of hydrodynamic models.

The microFloat, a new sensing system evelopped by the Applied Physics Laboratory (APL), has the potential to provide cost-effective, spatially-distributed resource assessments in tidal, river, and ocean energy applications. The microFloats use a buoyancy engine to move to and hold depth while otherwise drifting with the surrounding currents. An array of GPS-equipped surface buoys transmitting coded acoustic pings provides subsurface localization every 10 seconds. By simultaneously deploying a swarm of twenty floats, programmed to a range of depths, the system can map horizontal and vertical distributions of currents in the region of interest, with resolution depending on region width (cross-current) and depth. Developed specifically for economic distributed sensing, the total system cost is around $75k, approximately equal to the cost of two acoustic Doppler current profilers.

In August 2020, APL performed the first full-scale field trial in Agate Pass, WA, an energetic tidal channel with currents exceeding 2 m/s during testing. Over two days, seventeen twenty-minute surveys were gathered, each with 18-20 microFloats and five surface buoys. Two additional validation data sets were gathered during these surveys: (1) a vessel-mounted acoustic Doppler current profiler (ADCP) provided station-keeping data at three locations mid-channel during each survey; (2) four drifting buoys equipped with downward-facing ADCPs, called SWIFTs (Thomson et al. 2019), were deployed with microFloats. Results showed the float swarm's ability to simultaneously capture vertical and horizontal distributions of water velocity, providing improved spatial coverage over both ADCP platforms. Pointwise comparison of water velocity measurements between the float swarm and ADCPs agreed to within 12% of the nominal velocity, confirming that the floats are accurately resolving the tidal currents (Harrison et al. 2023b).

This project evaluated the utility of microFloat measurements in model refinement and validation. Researchers at Pacific Northwest National Laboratory (PNNL) previously developed a high-resolution hydrodynamic model of Puget Sound, WA, as published in Yang et al. (2021), which includes the Agate Pass test region within its domain. This model has been validated using stationary ADCP data collected by NOAA CO-OPS in selected areas of Puget Sound and represents the state of the art for site selection in this region. Under this support, PNNL refined a high-resolution subdomain model of Agate Pass. Field data from both microFloats and co-deployed instruments (drifting and stationary ADCPs) were used to validate this local-scale subdomain model and evaluated to assess how data from float swarms could be best used to increase model fidelity and the accuracy of annual energy production estimates.

2 Roles and Responsibilities of Project Participants

2.1 Applicant Responsibilities and Tasks Performed

APL provided PNNL with field data from the Agate Pass deployments, including data from the microFloats and co-deployed ADCPs (both stationary and drifting). Following refinement of the hydrodynamic model, APL assisted PNNL in analysis of the results and drafted a manuscript describing how microFloat observations can be used for model validation.

2.2 Network Facility Responsibilities and Tasks Performed

PNNL refined their Puget Sound hydrodynamic model in the Agate Pass subdomain to produce high resolution, four-dimensional hindcasts of tidal currents through Agate Pass, WA over the August 2020 microFloat field campaign survey period. PNNL used the field data to further validate the local-scale hydrodynamic model. The model outputs were generated at 30-second temporal resolution over the two days during which the field campaign took place. PNNL assisted APL in analysis of the results and aided in drafting a manuscript.

3 Project Objectives

The microFloats are currently high-level prototypes actively undergoing field testing (TRL6/7). Commercial viability (TRL9) and community acceptance can only be achieved through multiple rounds of field validation against standard instrumentation (e.g., ADCPs) in a variety of tidal conditions, as we have begun doing in Agate Pass.

The objective of this study was to evaluate the utility of high-resolution, spatially distributed field data, such as that provided by the microFloats, in refining site-scale hydrodynamic simulations of tidal channels and improving the accuracy of tidal energy production estimates. Improvement of the hydrodynamic model in the Agate Pass subdomain through a rigorous model validation process using a variety of field observations (microFloat, stationary ADCP, and drifting ADCP) provided direct insight into the spatial accuracy of the hydrodynamic model and how model accuracy may be improved by field data, especially microFloat data. In addition, these cross-validation results provided guidance for increasing microFloat data effectiveness through operation and post-processing improvements, and thus advance the TRL of the microFloat system.

4 Test Facility, Equipment, Software, and Technical Expertise

Numerical simulations of tidal hydrodynamics in Agate Pass were conducted at PNNL's Institutional Computing facility (PIC), overseen by Dr. Zhaoqing Yang. Led by Dr. Yang, PNNL's modeling team has extensive experience conducting tidal hydrodynamic modeling in many estuaries and coastal bays, including the Salish Sea. Model output of Agate Pass is in NetCDF format. All data has been archived and made available to the project team for analysis related to the project.

5 TEST OR ANALYSIS ARTICLE DESCRIPTION

The microFloat system comprises a swarm of twenty microFloats (as pictured being deployed in Figure 1a) and five surface localization buoys. The microFloats are equipped with a high-volume buoyancy-engine that provides a 9% density change, enabling automatic ballasting, vertical control from fresh to salt water (~3% density change) and reserve capacity for external sensors (e.g., hydrophones for acoustic monitoring). Using their buoyancy engine, the microFloats can move to and hold target depths, while otherwise drifting with the surrounding currents. GPS-tracked surface localization buoys broadcast coded acoustic messages to the subsurface microFloats, which record and timestamp these messages. Float position and velocity are calculated from these messages in post processing. This concept is depicted in Figure 2. By simultaneously deploying a swarm of twenty floats, programmed to a range of depths, the system can simultaneously map horizontal and vertical distributions of currents in the region of interest, with resolution depending on region width (cross-current) and depth. Developed specifically for inexpensive distributed sensing, the total system cost is around $75k, approximately equal to the cost of two acoustic Doppler current profilers. This work will evaluate the value of microFloat data towards improvement of high-resolution, local-scale models of tidal channels for predicting tidal currents and estimating tidal energy production.

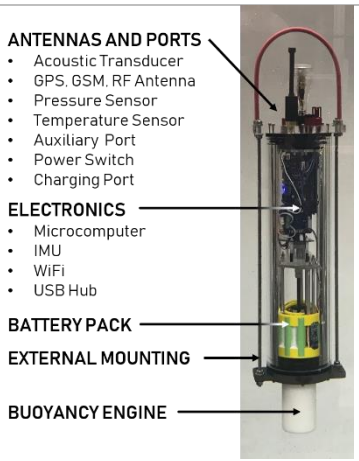

(a) microFloat subsystems

(b) Deploying a microFloat

Figure 1: Applied Physics Laboratory's microFloat

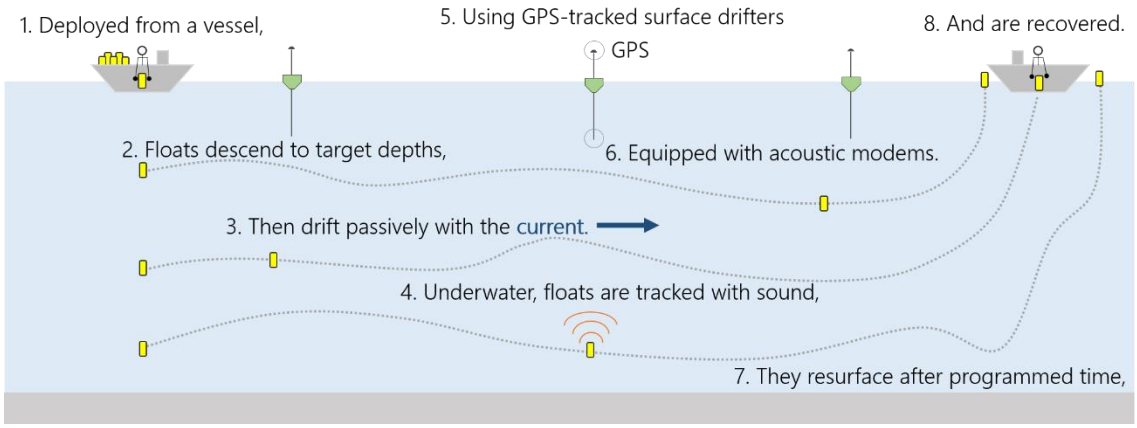

Figure 2: microFloat swarm sensing concept

6 Work Plan

6.1 Numerical Model Description

PNNL previously developed a regional-scale, time-resolved hydrodynamic simulation (FVCOM) of Puget Sound, WA, which includes the Agate Pass test region within its domain (Yang, et al. 2021). This model has been previously validated using stationary ADCP data collected by NOAA CO-OPS in selected areas of Puget Sound and represents the state of the art for tidal energy site selection in this region, with grid resolutions of 50 – 200 m in tidal channels. To be used for subsequent site-characterization, the model requires refinement and validation at local scales.

The project work plan consisted of four steps, with details provided in the following sections:

(1) Refinement of the Puget Sound hydrodynamic model in the Agate Pass region.
(2) Run a month-long tidal hydrodynamic simulation covering 18th and 20th August 2020.
(3) Validate the tidal hydrodynamic model for the Agate Pass subdomain using microFloat and ADCP field data.
(4) Cross-examine the refined hydrodynamic simulations.

6.1.1 Model refinement in Agate Pass region

The first task was to refine the hydrodynamic model grid in the Agate Pass region, with a horizontal grid resolution of 10-20 m. Model bathymetry in the Agate Pass region was re-interpolated from 2014 NOAA Puget Sound bathymetry dataset (NOAA 2014) and closely examined with new bathymetric data, e.g., 1-m USGS bathymetry in Puget Sound (Tyler, et al. 2020) and those obtained from the field measurements. The refined model grid for the Agate Pass region was incorporated into the Salish Sea model and set up with forcing (tides, wind, and river flows) for the August 2020 period.

6.1.2 *Run current simulations for 18th and 20th August 2020*

After refining the Agate Pass subdomain, tidal hydrodynamics (including water level and currents) were simulated for August 2020, corresponding to the previous field surveys with the microFloats and ADCPs which occurred on the 18th and 20th of August 2020. Horizontal velocities (*u* – east, *v* – north) were output at all grid locations (*x* – east, *y* – north, *z* – up) in the high-resolution subdomain, at 30-second resolution over each of the twenty-minute survey periods performed in the field experiment.

6.1.3 *Refined model validation using field data*

APL provided PNNL with field data from microFloats and ADCPs. Quality assurance of the field data had already occurred for the August 20th data set. Processing methods and results are included in Harrison et al. 2023a and Harrison et al. 2023b. microFloat data is restricted to horizontal velocity, while data from ADCPs (drifting and station-keeping) includes full three-dimension velocity (*u, v, w*). All data is horizontally geo-located and water-surface referenced.

6.1.4 *Cross-examination of refined Agate Pass models*

After the model refinement was completed and outputs generated, APL performed a cross-comparison of model outputs in collaboration with PNNL. Details of the evaluation are provided in Section 7.

Finally, APL and PNNL are actively drafting a joint publication on the methods and results of the analysis.

6.2 Test and Analysis Matrix and Schedule

	M1				*M2*				*M3*				*M4*				*M5*				*M6*			
Task	**WK 1**	**WK 2**	**WK 3**	**WK 4**	**WK 5**	**WK 6**	**WK 7**	**WK 8**	**WK 9**	**WK 10**	**WK 11**	**WK 12**	**WK 13**	**WK 14**	**WK 15**	**WK 16**	**WK 17**	**WK 18**	**WK 19**	**WK 20**	**WK 21**	**WK 22**	**WK 23**	**WK 24**
Refine Puget Sound hydrodynamic model in Agate Pass Region																								
Run tidal current simulations for Aug 2020																								
APL supplies microFloat and ADCP field data to PNNL																								
Refine tidal current simulations using field data																								
Cross-evaluate Agate Pass current simulations																								
Joint publication																								
Post Access Report																								
Post Access Questionnaire																								

PNNL Task

APL Task

Joint Task

6.3 SAFETY

As this project involves only numerical analysis, there were not specific safety protocols beyond the normal operational safety protocols employed by PNNL and APL.

6.4 CONTINGENCY PLANS

No contingency plans were pursued during the test.

6.5 DATA MANAGEMENT, PROCESSING, AND ANALYSIS

6.5.1 Data Management

MHK-DR submissions are summarized in Table 2.

Model data, both directly simulated and derived, have been stored in the PNNL PIC system. All data is in NetCDF or ASCII format.

Field data from the microFloats and ADCPs are stored on APL workstations and mirrored in cloud-based storage (Dropbox). An explanatory file (.pdf format) describes the survey and field data structure. Processed data is stored in .mat format, with one file for each survey from August 20th. This data includes:

- Survey summary: start time, number of floats, water level.
- microFloat data:
    - Cleaned data for each float in survey,
    - Time series of position (lat, lon), depth (relative to surface), and horizontal velocity (*u, v*)
- Drifting ADCP data
    - Cleaned data for each drifting ADCP in survey
    - Time series of position (lat, lon), sample depth (relative to surface), and observed water velocity (*u,v,w*)
- Stationary ADCP data
    - Cleaned data for each station-keeping data set in survey
    - Time series of position (lat, lon), sample depth (relative to surface), and observed water velocity (*u,v,w*)

Table 2: *MHK-DR submission summary*

FVCOM model outputs	Water level and velocity, as well as derived variables (e.g., power density) from the final refined model simulations for the Agate Pass subdomain	NetCDF and ASCII files for the duration of August 18th and 20th 2020 field surveys.
microFloat and ADCP field data	Horizontal velocity at each observation point from August 20th field surveys	.mat files for each platform .pdf data description .pdf processing description

6.5.2 Data Processing

Model results of water level and velocity were automatically output from model runs in NetCDF format and no post-processing is required. For cross-comparison, model results were interpolated at the same locations as field data for accurate model-data comparison. Because the model uses sigma-stretch coordinates, variation of sea surface and total water depth were taken into account.

Processing and analysis of the microFloat and ADCP field data from Agate Pass was performed prior to the TEAMER project and has been recently published in Harrison et al. 2023a and 2023b.

6.5.3 Data Analysis

To compare the high-resolution Agate Pass subdomain data to the field observations, the following data analysis was performed.

1. To verify the refined model, water level and currents were compared against established NOAA data products: tidal gauge at Bremerton and an ADCP bottom-lander deployment from 2015.
2. From the refined Agate Pass subdomain, we interpolated the horizontal distribution of depth-averaged horizontal water currents and depth-averaged power density ($P = \frac{1}{2}\rho U^3$) for each survey period.
3. Similar to analysis 1, distributions of tidal currents and power density along a vertical plane roughly following the thalweg of Agate Pass channel were plotted to assess changes in vertical gradient mapping for all model refinements.
4. For a statistical assessment of refinements, all model outputs were interpolated at field data points for all August 20th surveys. The difference between simulated and observed horizontal velocities for each platform were computed, with percentile-based (10th, 25th, 50th, 75th, and 90th) distributions reported.
5. To better assess sources of model-observation discrepancies, we generated the same model-observation distributions (Analysis 4), given (1) time-averaging the model and/or observations; (2) time-shifting the model and observations.

Scripts to perform this analysis are included in the MHK-DR submission, along with explanatory text.

7 PROJECT OUTCOMES

7.1 RESULTS

7.1.1 Model Refinement

As outlined in the Work Plan (6.1.1), the first task was the refinement of the Puget Sound hydrodynamic model in the Agate Pass region. Figure 1 compares the FVCOM hydrodynamic model mesh used in the Salish Sea tidal energy resource characterization study (Yang et al., 2020, 2021) and the newly refined version used for this study. The spatial resolution in the Agate Pass region was significantly improved to provide a more detailed representation of the geometric features of the study area. More specifically, the refined grid in Agate Pass has a spatial resolution of 15-20 meters (in terms of the triangular grid side length), which is about 1/3 of the resolution (i.e., side length) used in the 2021 study. The refined grid resolution of 15-20 meters is close to the resolution of the 10-m high-resolution bathymetry dataset obtained from NOAA. 20 terrain-following, uniformly distributed sigma layers were used to resolve the vertical flow structure. This configuration is the same as the previous study (Yang et al., 2020, 2021).

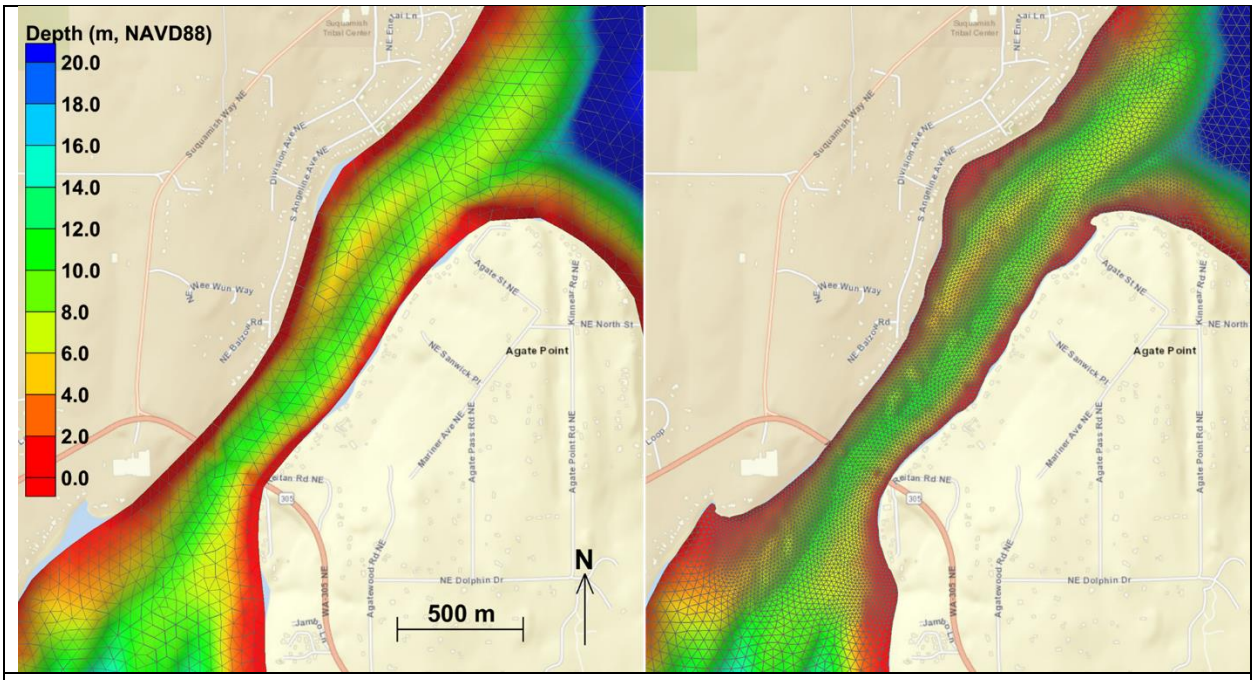

Figure 1: A comparison of the original mesh (left panel) and the refined version (right panel) for the Agate Pass region.

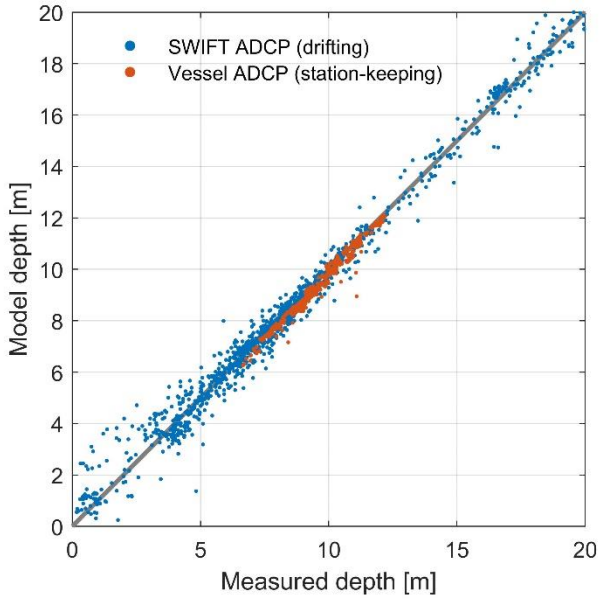

Figure 2: Comparison of model depth versus depth measured by ADCP devices.

To confirm model bathymetry matched the real bathymetry, we compared measurements of water depth to co-located positions in the model (Figure 2). Agate Pass was sufficiently shallow such that both SWIFT and vessel ADCPs could measure water depth throughout the deployment. For each horizontal location (x,y) and time (t) of an ADCP-based depth measurement, we computed the corresponding model water depth. Model depth is computed as the addition of the static depth (relative to MLLW) plus the time-varying water level, both linearly interpolated in space (and in time for water level). The mean difference between SWIFT and model values was 0.03 m, while the mean difference between vessel ADCP and model values was 0.1 m. These comparisons verified that the model bathymetry accurately represented the site.

In previous modeling studies, tidal validation inside West Sound (the area consisting of those multiple bays and inlets behind Agate Pass and Rich Passage) was either achieved through comparing FVCOM predictions against harmonic tidal predictions downloaded from NOAA and XTide websites or simply neglected due to lack of field observations (Yang et al., 2020 and 2021). Starting from summer 2021, NOAA tidal observations became available at the Bremerton tidal station. Therefore, we specifically configured the model for August 2021 to confirm if the model can accurately reproduce the observed water level at the Bremerton tidal gauge. Figure 3 shows the time series comparisons of FVCOM predicted water level and NOAA observations. The comparisons are very reasonable with root-mean-square-error (RMSE) of 0.102 m and Pearson correlation coefficient of 0.997.

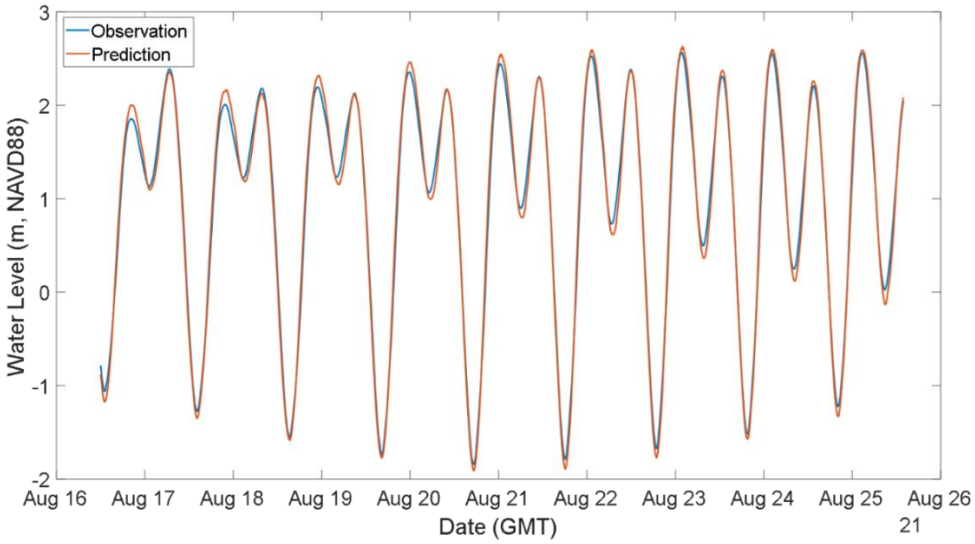

Figure 3. Water level validation at NOAA Bremerton tidal gauge for August 2021.

In addition to water level validation, we also rechecked model performance in simulating tidal currents using NOAA's 2015 current survey data in Agate Pass at Station PUG1501[1] (Figure 4). Comparisons of scatter points between modeled and observed velocities (Figure 5) indicates that the model successfully reproduced the current magnitude and direction in the Agate Passage, although slight differences in magnitude and direction are observed. However, such differences are well within the error criteria defined by NOAA (Hess et al. 2003). Based on NOAA's standards, the accepted RMSE errors for current speed and current direction are 0.26 m/s and 22.5°, respectively. Our model results show that the RMSE errors for current speed and direction are 0.168 m/s and 8° respectively, which are well within the NOAA recommended error criteria.

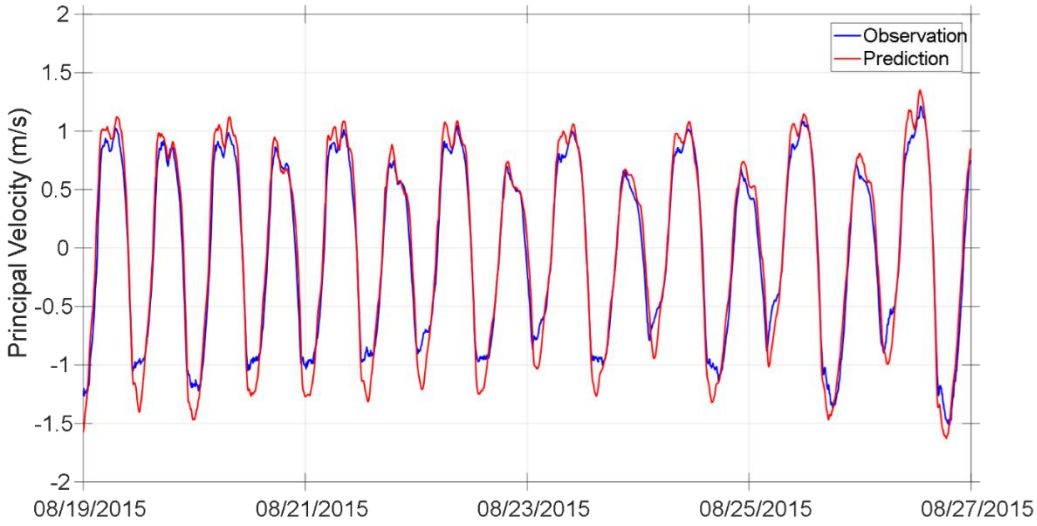

Figure 4. Timeseries comparison of depth-averaged current velocities between model predictions and field observations at NOAA C-MIST Station PUG1501. Negative values are southwestward flows, I.e., flood currents.

[1] https://cmist.noaa.gov/cmist/requests/selectdata.do?stationid=PUG1501

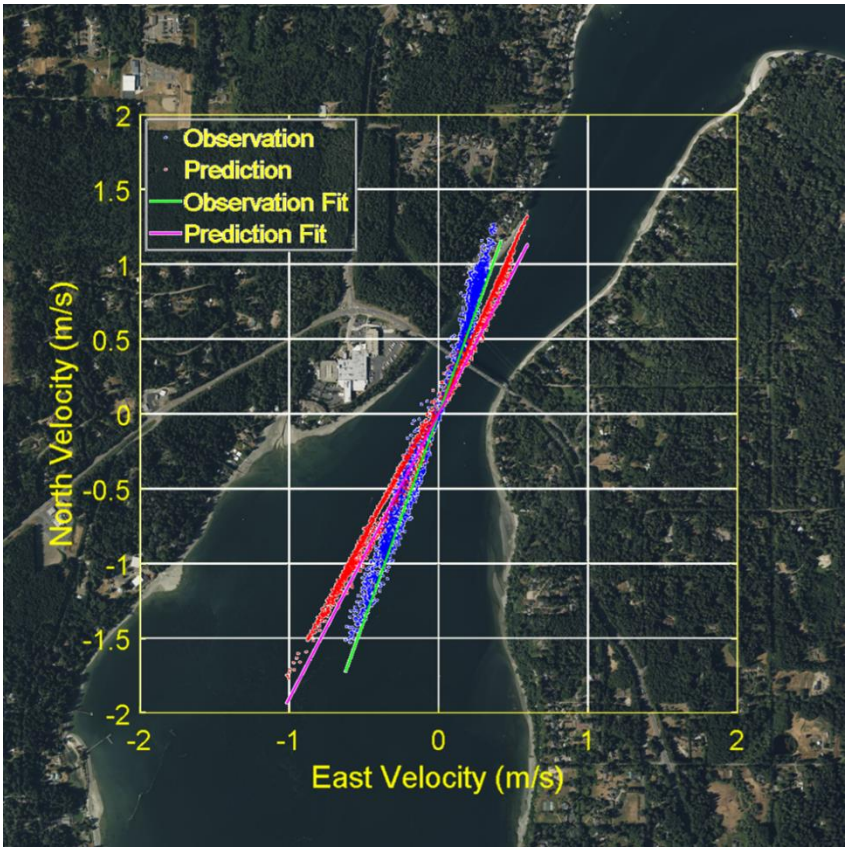

Figure 5: Scatterpoint comparisons of depth-averaged velocities between model predictions and field measurements at NOAA C-MIST Station PUG1501 (the station is located right at the origin of the Axis). The angle between predicted and observed principal directions is about 8°.

Figure 4 shows the time series comparison of depth-averaged velocities that were projected onto respective principal axes of model predictions and field observations (Figure 5). The model reproduces observed currents very well in both magnitude and phase except for slight overprediction in peak current magnitudes.

Table 1 shows the error statistics for velocity predictions, which are overall better than those in the previous study (Yang et al., 2021), confirming the Puget Sound model in Agate Pass is improved after grid refinement.

Table 1: Error statistics of model predicted, depth-averaged current velocities at NOAA C-MIST Station PUG1501. SI stands for scatter index and R stands for Pearson correlation coefficient.

Error Stats	East Velocity	North Velocity	Principal Velocity
RMSE (m/s)	0.160	0.132	0.168
SI (%)	65.1	19.3	23.1
R	0.980	0.988	0.987

Figure 6 compares the 2-D velocity profiles between model and data at Station PUG1501, illustrating the model reproduces observed velocity profiles in both time and space/depth. It should be mentioned that ADCP observations typically only capture the middle portion of the water column, while model predictions can cover the entire water column.

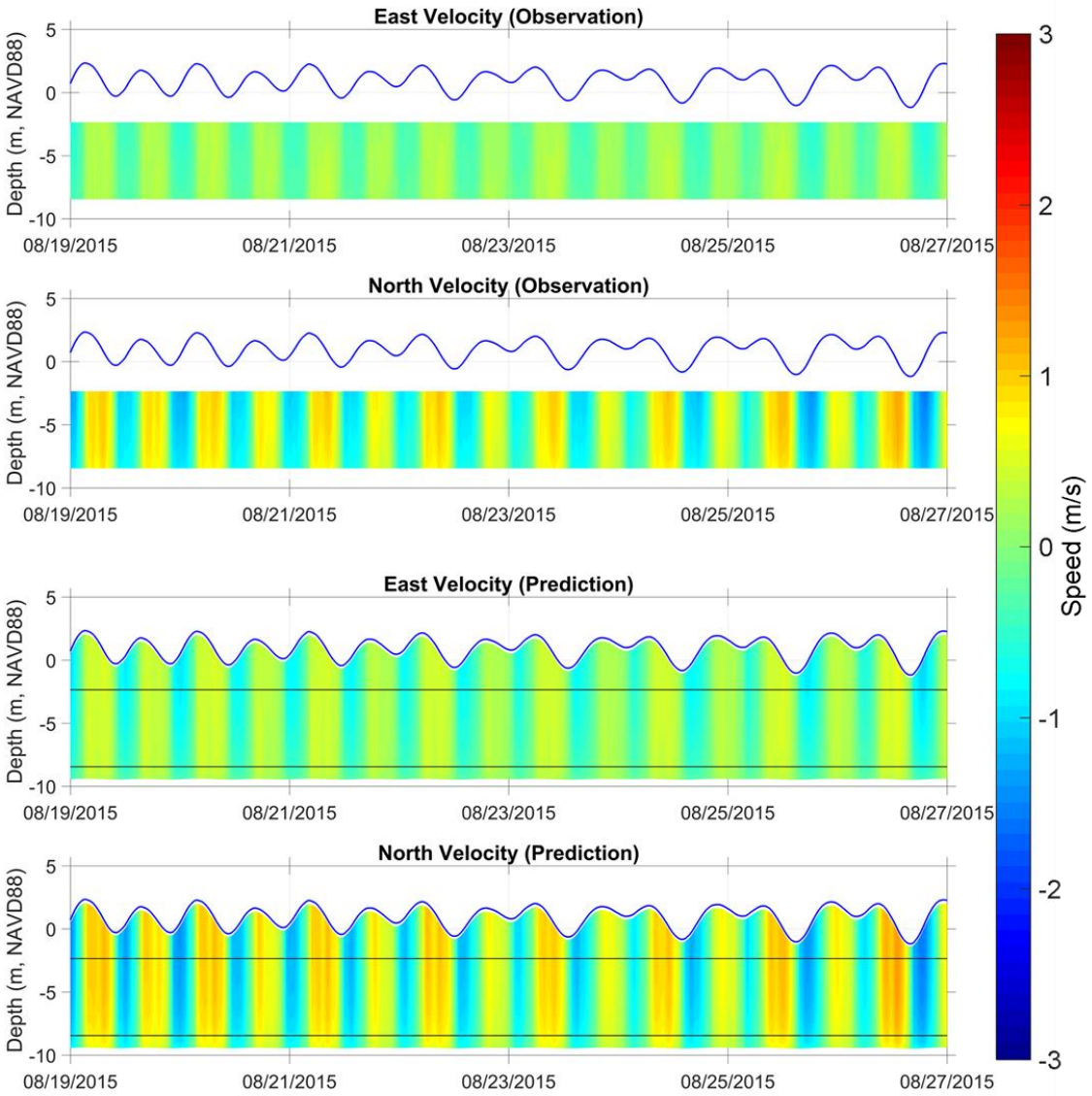

Figure 6: 2-D velocity profile comparisons between field observations (top two panels) and model predictions (bottom two panels) at NOAA C-MIST Station PUG1501, illustrating the model was capable of reproducing observations in both time and space (depth).

7.1.2 Tidal Hydrodynamics in Agate Pass

Once the hydrodynamic model was successfully refined and improved, we used the model output to assess the current and power density distributions in the Agate Pass area. Figure 7 shows the instantaneous depth-averaged current field at both peak ebb and flood during the August 20, 2020 microFloat survey period. Figure 8 shows the corresponding power density field. The results suggest that Agate Pass is flood-dominated, i.e., both current and power density magnitude at peak flood is stronger than that at peak ebb.

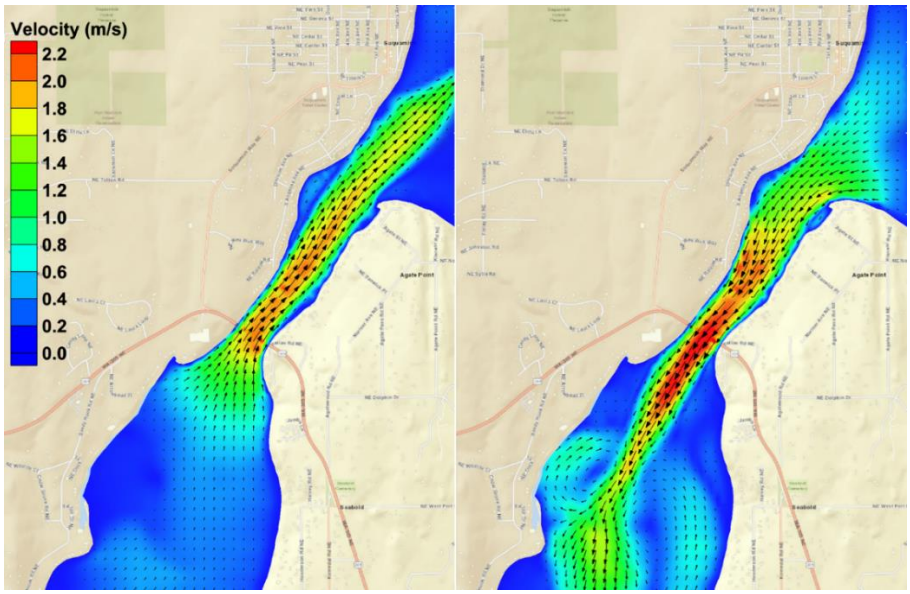

Figure 7: Model predicted instantaneous depth-averaged current field at peak ebb (left panel) and flood (right panel) on August 20, 2020.

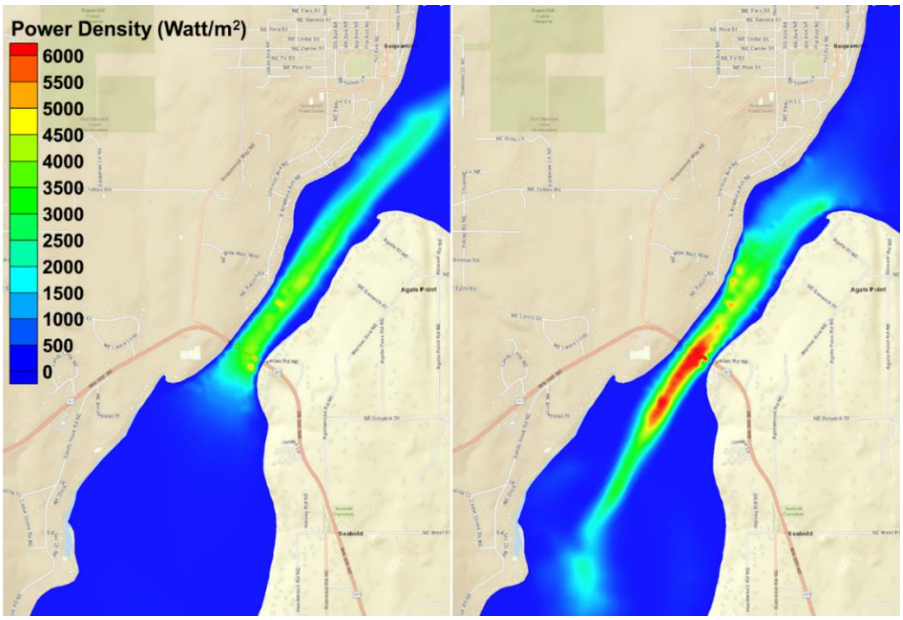

Figure 8: Model predicted instantaneous depth-averaged power density at peak ebb (left panel) and flood (right panel) on August 20, 2020.

We further checked the 2-D current and power density profiles along the longitudinal transect of Agate Pass (Figure 9). The model results of current (Figures 10) and power density (Figure 11) confirmed the flood dominance suggested in the depth-averaged plots. For instance, the peak ebb current magnitude and power density reach 3 m/s and 10 kW/m^2, respectively toward the surface near Agate Pass Bridge. Note that the legends in Figures 10 and 11 are different.

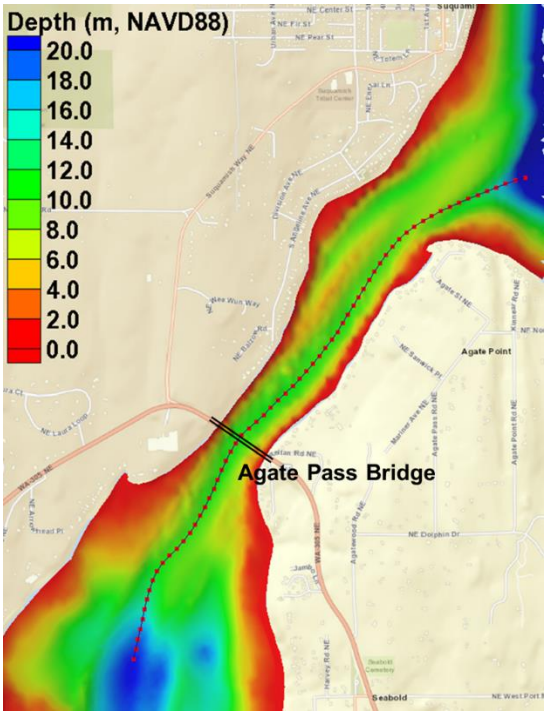

Figure 9: The transect line along the thalweg of Agate Pass.

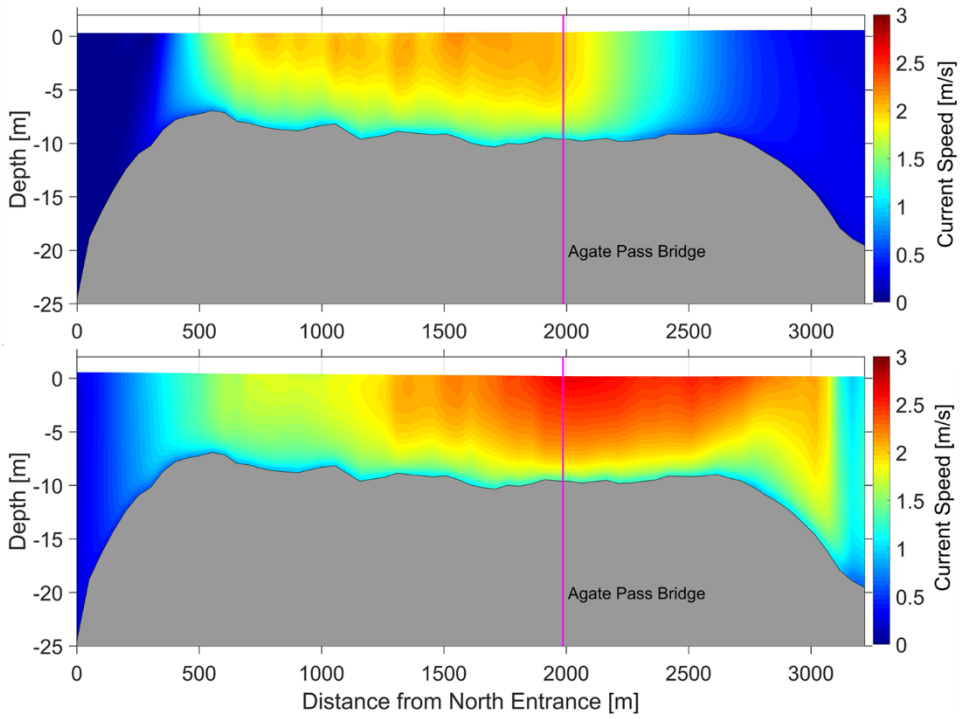

Figure 10: Instantaneous current profile at peak ebb (top panel) and flood (bottom panel) along the transect line in Figure 9 on August 20, 2020.

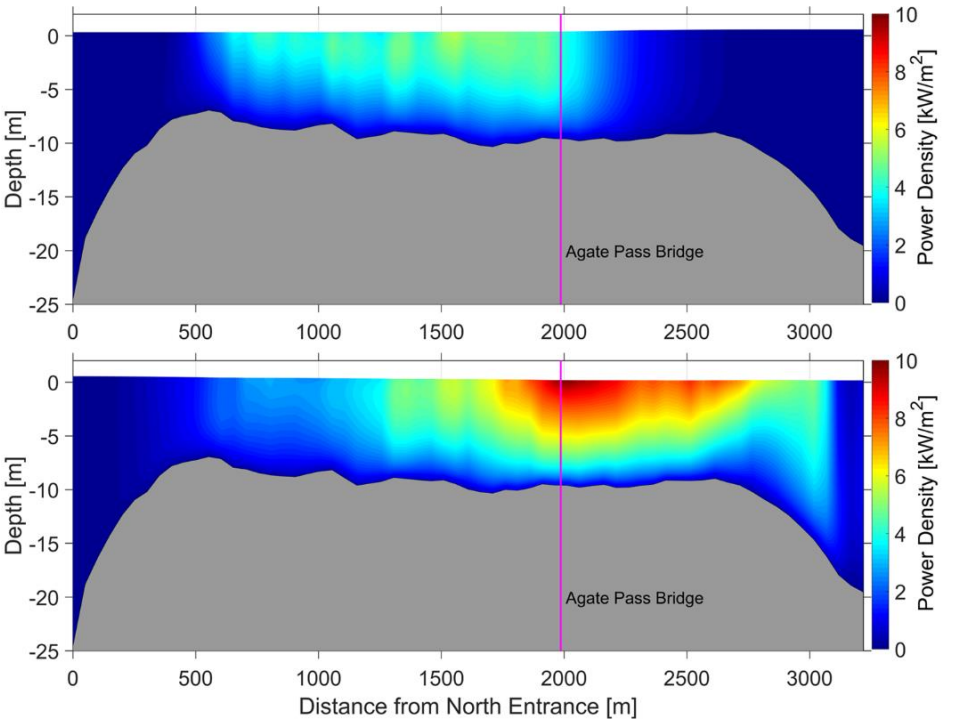

Figure 11: Instantaneous power density profile at peak ebb (top panel) and flood (bottom panel) along the transect line in Figure 9 on August 20, 2020.

7.1.3 Model Validation with microFloat Data

Through the remainder of the results, we make references to survey periods pictured in Figure 12. Note that surveys 1-4 occurred during the ebb tide (with E4 at essentially slack tide) and surveys 5-9 (i.e., F1 - F5) occurred during flood tide.

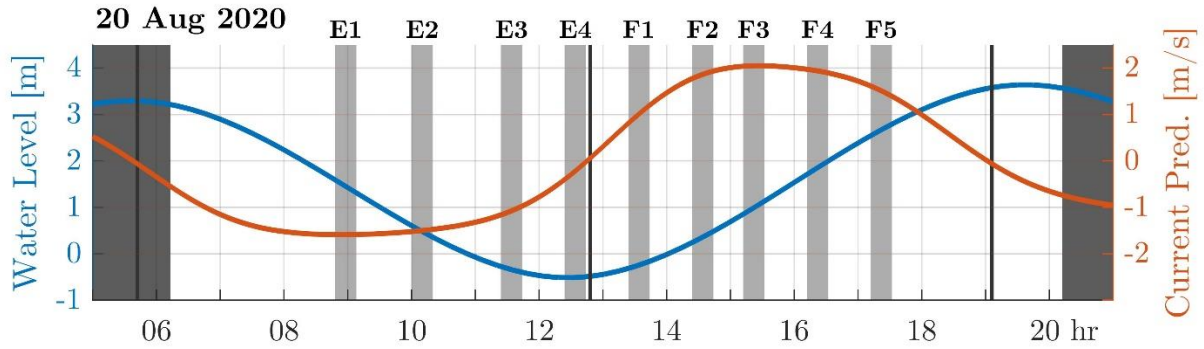

Figure 12: Survey periods (indicated in light grey) for the field data, with predicted water level and tidal currents over the test day. Dark grey vertical lines indicate slack tide. (Figure originally published in Harrison et al. 2023b.)

To evaluate the hydrodynamic model performance using microFloat data, we first compared model predicted trajectories against microFloat field measurements. We utilized the built-in particle trajectory module in FVCOM to simulate microFloat trajectories during the August 20, 2020 survey, initializing the trajectory simulations at the microFloat released locations. Comparisons of selected microFloat trajectories are shown in Figures 13-16. Overall, model predictions agree with measurements in the trajectory, despite increasing discrepancy with elapsed time. These results are consistent with the comparisons of 2-D scatter plots between modeled and NOAA observed velocities, as shown in Figure 4. Figures 13-16 demonstrate that the microFloat trajectories are a valuable dataset that can be used to validate tidal hydrodynamic models.

The discrepancy in travel distances observed in trajectory comparisons (Figs.13-16) agree with the overall difference in horizontal current magnitudes (Fig 19): in Survey 2 (E2), predicted currents are slightly stronger than observed, while in Survey 9 (F5), predicted currents are considerable slower than observed. Misalignment between the trajectory directions is also consistent with the misalignment observed in the fixed station velocity comparisons at NOAA C-MIST Station PUG1501 in Figure 4.

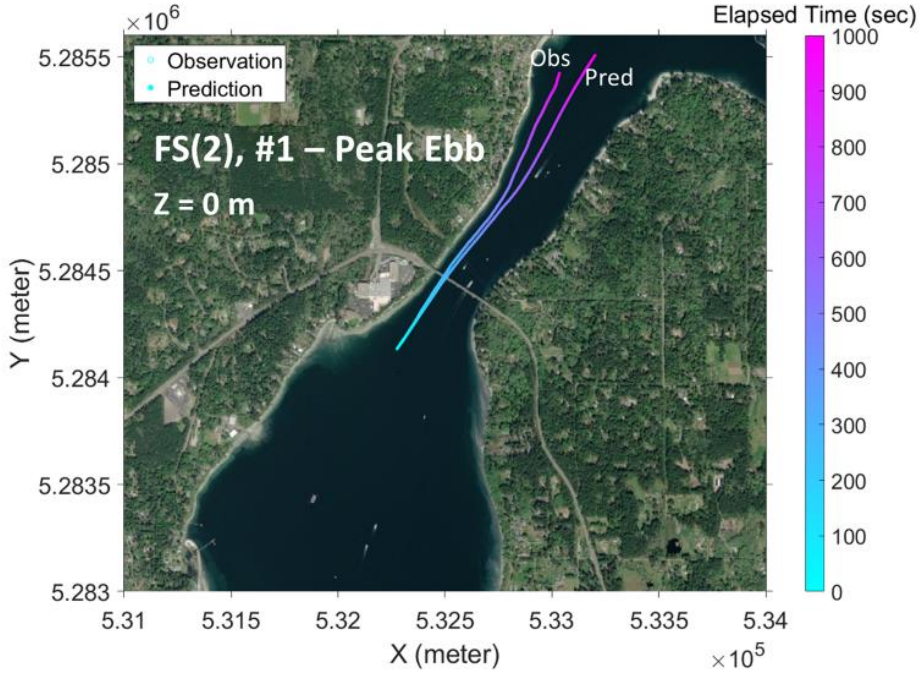

Figure 13: Model simulated particle trajectory vs. measured microFloat trajectory for microFloat #1 deployed during the ebb tide (E2) on August 20, 2020.

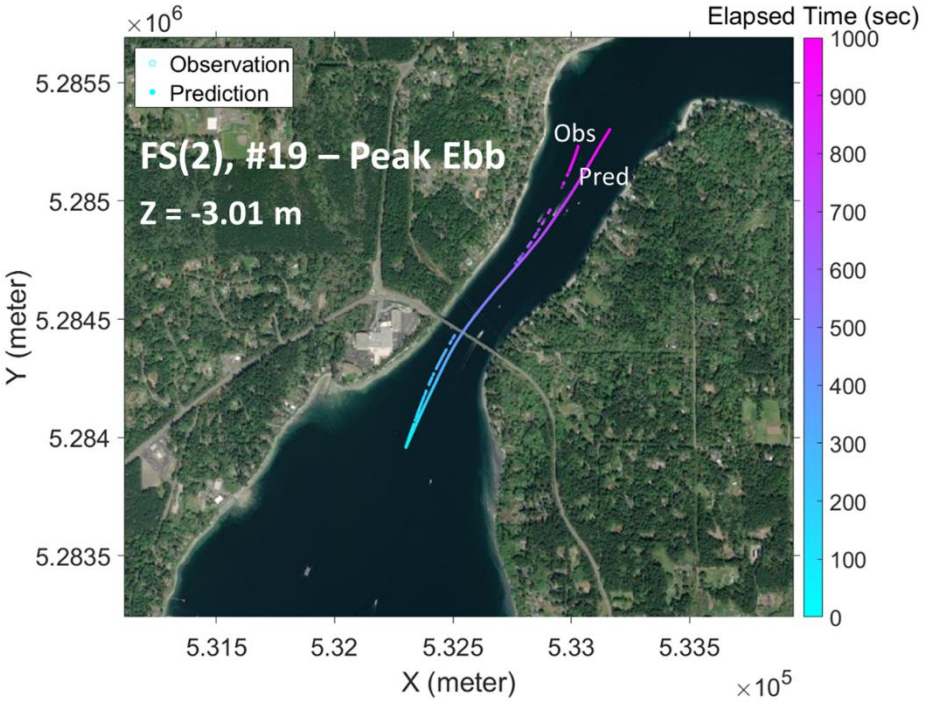

Figure 14: Model simulated particle trajectory vs. measured microFloat trajectory for microFloat #19 deployed during the ebb tide (E2) on August 20, 2020.

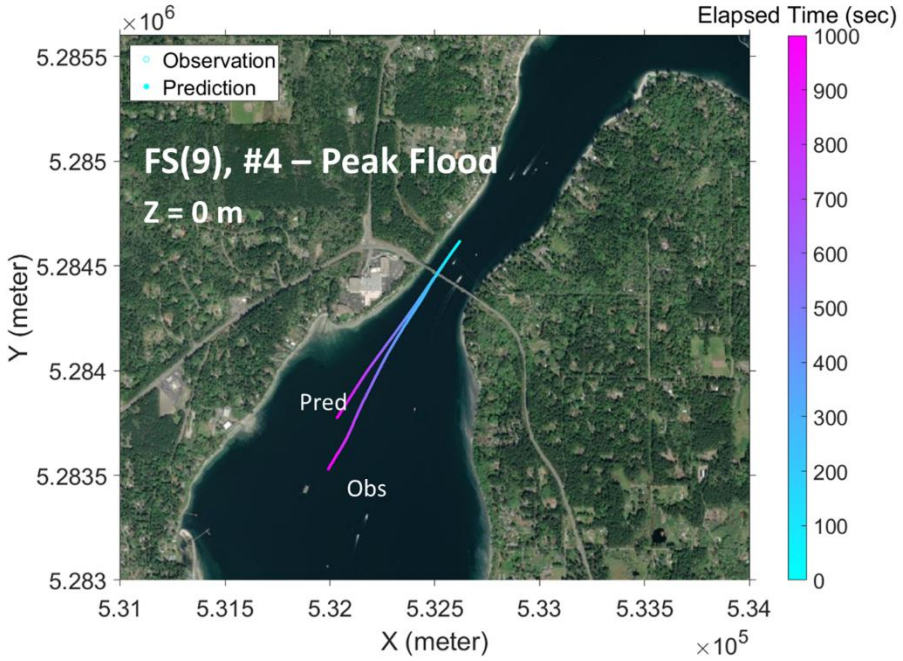

Figure 15: Model simulated particle trajectory vs. measured microFloat trajectory for microFloat #4 deployed during the flood tide (F5) on August 20, 2020.

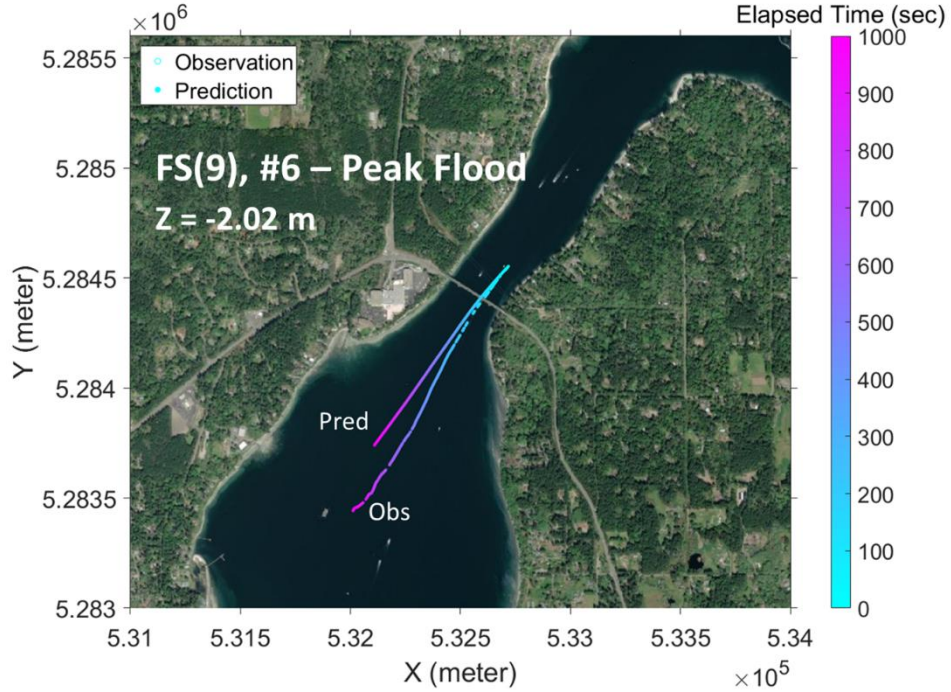

Figure 16: Model simulated particle trajectory vs. measured microFloat trajectory for microFloat #6 deployed during the flood tide (F5) on August 20, 2020.

To further assess agreement between the model and the observations on a granular level, we interpolated the simulation results in space and time at the location (*x, y, z, t*) of each observation point. Each of the nine surveys (Figure 12) that occurred on August 20th were assessed independently. Here, we include visualizations of the comparison of horizontal velocity U_H magnitude for two surveys, one during the tidal ebb (Survey E2, Figure 17) and one during the flood (Survey F3, Figure 18).

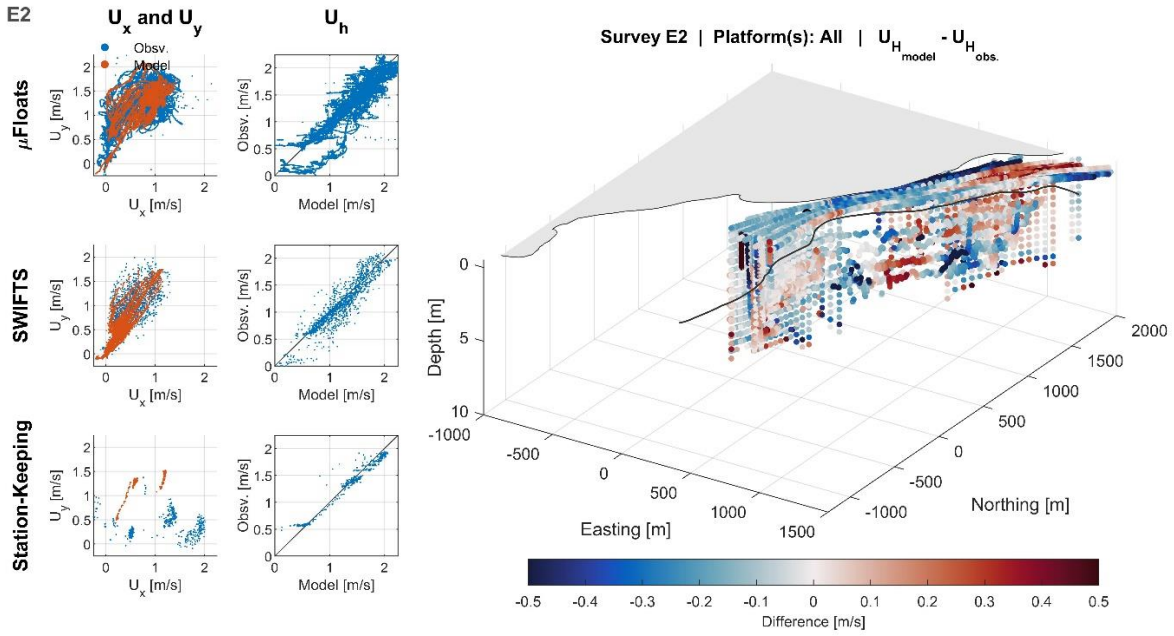

Figure 17: Comparison between modelled and observed velocities for ebb tide survey E2.

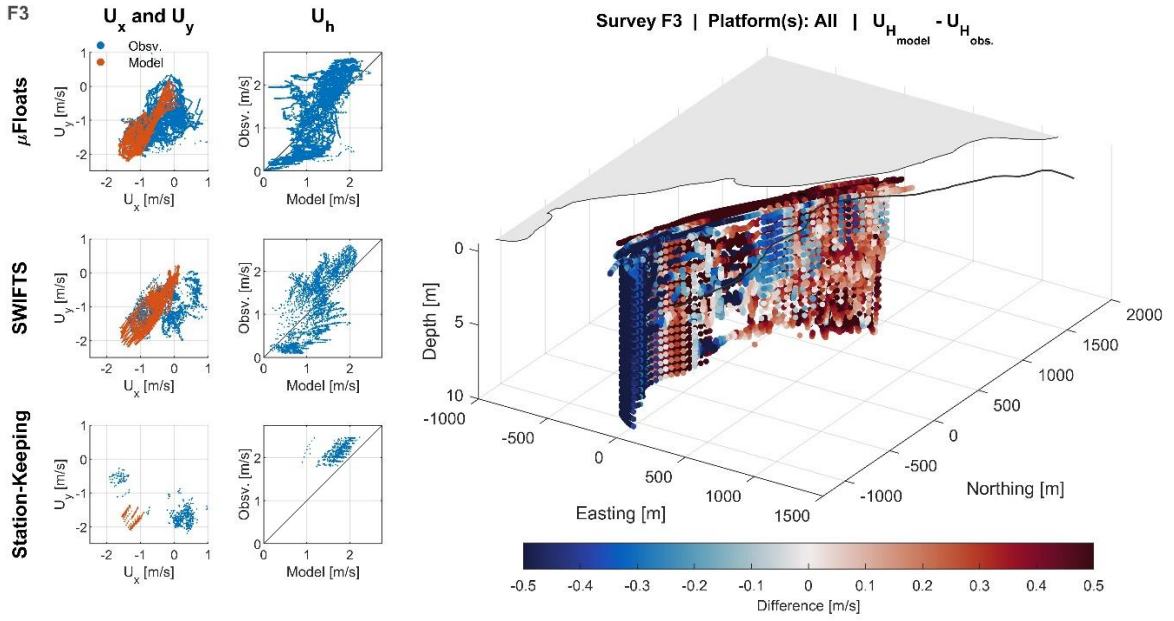

Figure 18: Comparison between modelled and observed velocities for flood tide survey F3.

These two examples typify differences between ebb and flood deployments, most noticeably that the simulations and field observations exhibited much closer agreement for ebb surveys than for flood surveys. Looking across all surveys, we were unable to distinguish a consistent spatial pattern of error.

To further assess the source of model-data differences, we performed two modifications of the point-wise comparison: (1) averaging the model and observation data; (2) time-shifting the model and observation data.

If the predominant source of model-data difference results from high-frequency fluctuations in the observations (e.g., from turbulence or measurement noise), averaging the observations should improve the agreement. microFloat data, with a starting resolution of 1 s, was window-averaged over 30 s, 60 s, and 120 s periods. The sample position (*x,y,z,t*) was also averaged over the same interval. Note that at a nominal velocity of 1 m/s, this spatially averages over 30 m, 60 m, and 120 m horizontally for the given window sizes. A reminder that the horizontal resolution of the model element size is 15-20 m. Along with smoothing (i.e., averaging) the field observations, we also evaluated the impact of averaging the model data using 60 s, 120 s, and 300 s windows. To compare errors across survey, observation type, model averaging window, and observation averaging window, we computed a seven-number distribution of model-data differences (10^{th}, 25^{th}, 50^{th}, 75^{th}, and 90^{th} percentiles) for each realization, as pictured in Figure 19.

Examining the results from this averaging analysis, we observe the following trends:

(1) Time-averaging the model data has negligible impact on intercomparisons across all instruments, tidal stages, and levels of time-averaging the field data.
(2) Time-averaging the field observations results in small, but noticeable reductions in the distribution width for float and SWIFT ebb observations. For float observations during flood deployments, the impact is less pronounced. Interestingly, SWIFT observations during the accelerating flood (F1 though F3) appear to exhibit greater difference from the model upon averaging, which is unexpected. The impact of averaging on station-keeping data is quite small.

In addition to time-averaging the data, we examined the impact of time-shifting the observation data relative to the model time step from -15 minutes to +15 minutes at one-minute increments. We used the same difference distributions computed for the averaging procedure to evaluate time-shifting impacts, with compiled results pictured in Figure 20.

The time-shifting results did not reveal a consistent relationship between an optimal time shift (defined as the time-shift that minimized the magnitude of the median difference for a given device and survey). This suggests that differences between simulated and observed currents are not due to temporal misalignment. In general, the distribution width doesn't change considerably with time-shifting. The exceptions, E4 and F1, are the survey periods around slack tide, which likely experience overall changes in the flow structure, as opposed to periods of established flow pattern with moderate changes in magnitude. This result suggests that the interquartile and interdecile ranges are primarily driven by spatial effects and noise, errors, and/or turbulence in observations.

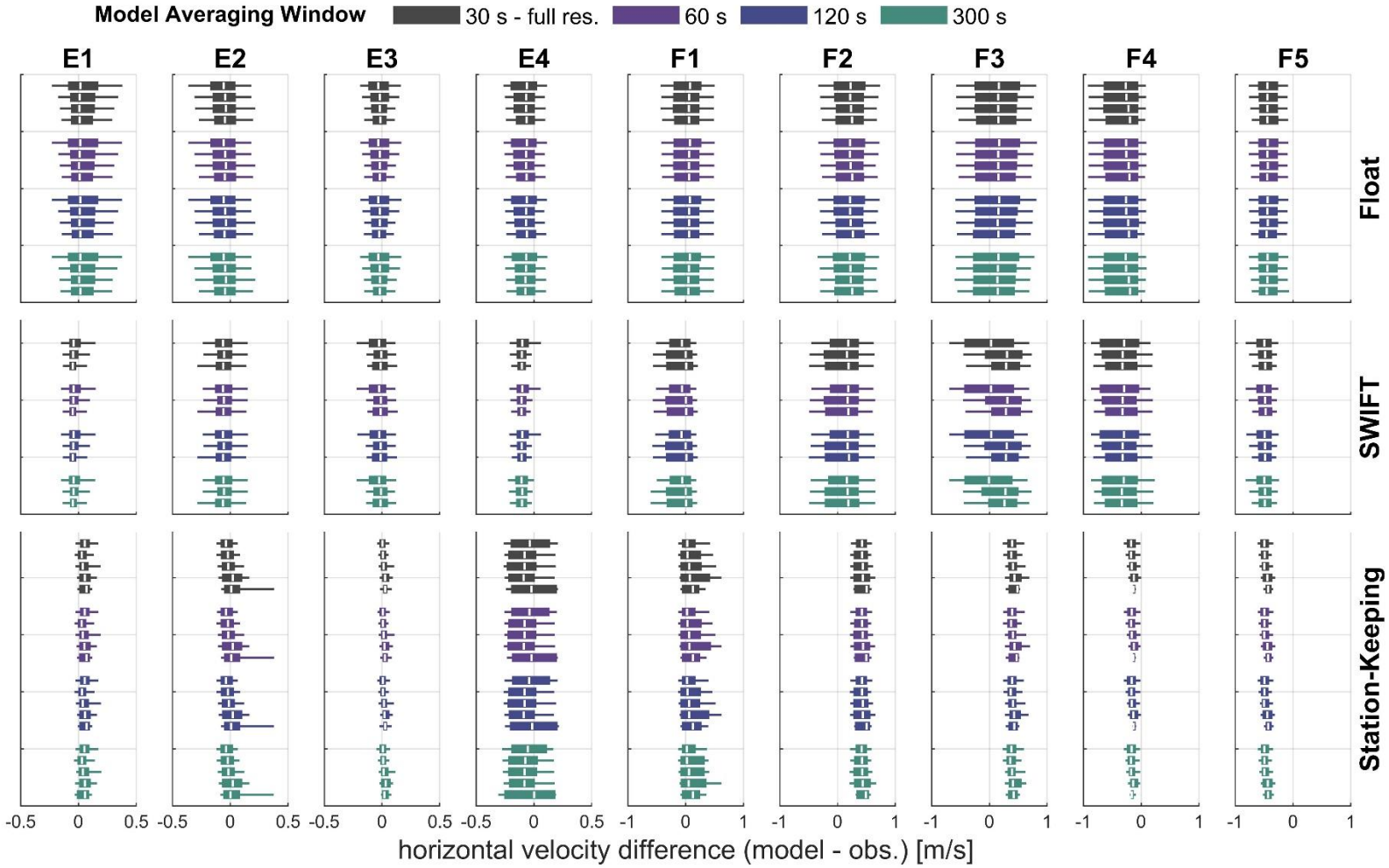

Figure 19: Distributions of differences between model and field data, computed across all surveys and instruments, for each combination of field data and model averaging. Color encodes model averaging. Each grouping of the same color includes differing levels of averaging the field data, arranged, top to bottom, from highest resolution (no averaging) to lowest resolution (most averaging) for that instrument. For float data: 1 s (full resolution), 30 s, 60 s, and 120 s. For SWIFT data: 30 s (full resolution), 60 s, and 120 s. For station-keeping data: 15 s (full resolution), 30 s, 60 s, 120 s, and 300 s.

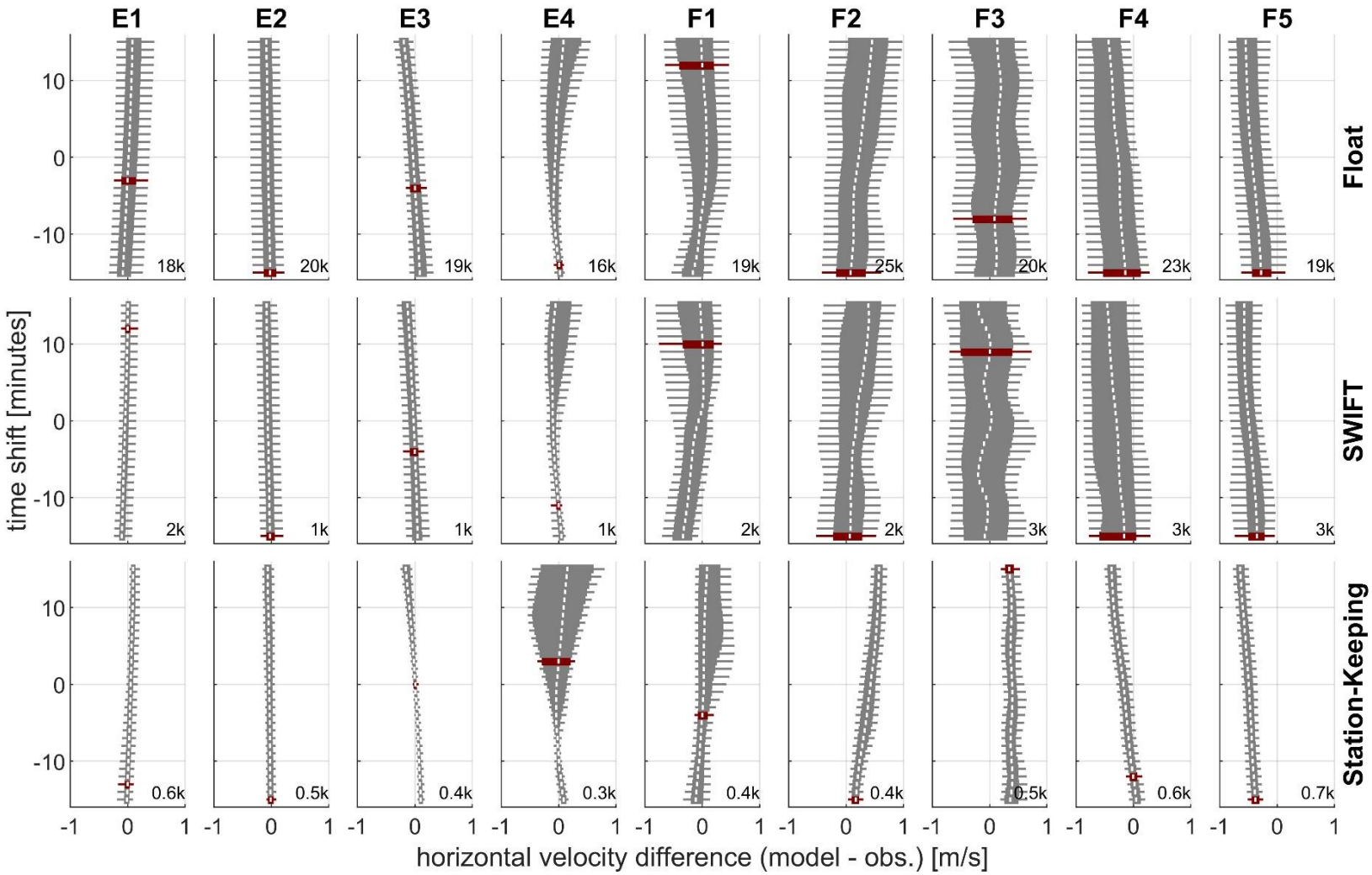

Figure 20: Distributions of differences between model and field data, computed across all surveys and instruments, with field observations time-shifted relative to the model. A negative time-shift indicates the field observation being compared to an earlier-than-true model time step. The number in the bottom right corner of each subplot indicates the number of samples for that instrument and survey. The distribution highlighted in red indicates the time-shift with the minimum magnitude difference between model and observation.

Overall, model results agree with microFloat observations, although there is considerably better agreement between model and field observations during ebb tide conditions than during flood. We hypothesize that this is due to the location of the field observations relative to spatially constrained vs. unconstrained flow. During ebb deployments, observations were primarily restricted to the channel. During flood deployments, the observations extend from within the channel out into the body of Port Orchard, primarily carried by a jet. While, the model captures the presence of the jet (Figure 8), the exact location is unlikely to match reality, resulting in differences between model and observation.

7.2 Lesson Learned and Test Plan Deviation

APL researchers were leveraging time on a separate project that this work semi-directly supported. However, lack of specific*, designated funding* to perform the data analysis and writing steps delayed completion of the project. We should not have included the paper writing and submission as part of the original proposal. Such an effort should be supported by additional "follow-on" funds (for *both* applicant and recipient), where project outcomes are well-suited for publication.

Two changes were made to the data analysis efforts:

1. The scaffolded processing strategy proposed (originally in Section 6.1.3) was not utilized as the hydrodynamic modeling method was not suitable for such true "assimilation"-based refinement. As such, only *comparisons* between model and field data were pursued. After the original round of refinement and comparison with the field data, a single additional refinement was undertaken, however this negligibly impacted the model-field data comparisons.
2. In evaluating comparisons, APL discovered data quality issues with the field observations unknown prior to the start of the TEAMER project. These were: (1) Localization of the microFloats on Aug 18th were insufficient to produce quality tracks and velocity measures; (2) two SWIFTS did not record on Aug 18th; (3) an error in the station-keeping ADCP compass resulted in erroneous velocity directions (magnitudes were correct). As such, data from Aug 18th was not used for comparisons and station-keeping direction data not evaluated for comparisons. For future work with ADCPs, users should be aware that mounting the ADCP with the beams offset 45° from primary direction of flow is recommended for improved data quality.

8 Conclusions and Recommendations

The project provided an excellent opportunity to evaluate how high-resolution, spatially distributed data from microFloat could be used to validate local-scale tidal hydrodynamic models. The methodology implemented in this study is straightforward and can be applied to future model-observation comparisons, although analysis of the results is complicated. The challenge comes in interpreting the differences observed, identifying plausible causes, and their implications for model fidelity. Ultimately, the field data set was sparse (i.e., too few and too short deployments) and the flow structure sufficiently complex such that drawing broadly applicable conclusions proved out of scope. To further the investigation, a bigger field observation data set would be needed, preferably multiple sequential tidal cycles (a few days) gathered over a minimum of two different periods of the lunar cycle. Ultimately, this work indicated that the microFloat data are cost-effective and extremely valuable in the absence of

ADCP data and can be used to support model validation for tidal energy resource characterization and assessment.

9 REFERENCES

Harrison, T., Crisp, C., Noe, J., Mundon, T., Neasham, J., Polagye, B. 2023a*: Adaptable Swarm Sensing in Coastal Waterways: Design and Performance of the μFloat System*. Field Robotics*,* 3, 516-543. https://doi.org/10.55417/fr.2023016

Harrison, T., N. Clemett, B. Polagye, and J. Thomson, 2023b: *Experimental Validation of Float Array Tidal Current Measurements in Agate Pass, Washington*. J. Atmos. Oceanic Technol., 40, 475–489, https://doi.org/10.1175/JTECH-D-22-0034.1.

Hess, K.W.; Gross, T.F.; Schmalz, R.A.; Kelley, J.G.W.; Aikman, F.; Wei, E.; Vincent, M.S. 2003. *NOS Standards for Evaluating Operational Nowcast and Forecast Hydrodynamic Model Systems*; NOAA Technical Report NOS CS 17; National Oceanic and Atmospheric Administration: Silver Spring, MD, USA.

NOAA 2014. *DEM Puget Sound 1/3 arc-second NAVD 88 Coastal Digital Elevation Model.* https://www.ncei.noaa.gov/access/metadata/landing-page/bin/iso?id=gov.noaa.ngdc.mgg.dem:5165

Thomson, J., Moulton, M., de Klerk, A., Talbert, J., Guerra, M., Kastner, S., Smith, M., Schwendeman, M., Zippel, S. and Nylund, S., 2019. *A new version of the SWIFT platform for waves, currents, and turbulence in the ocean surface layer*. 2019 IEEE/OES Twelfth Current, Waves and Turbulence Measurement (CWTM), San Diego, CA, USA, 2019, pp. 1-7, https://doi.org/10.1109/CWTM43797.2019.8955299

Tyler, D.J., Danielson, J.J., Grossman, E.E., and Hockenberry, R.J., 2020, *Topobathymetric Model of Puget Sound, Washington, 1887 to 2017*: U.S. Geological Survey data release, https://doi.org/10.5066/P95N6CIT.

Yang, Z., Wang, T., Branch, R., and Xiao, Z. 2020. *Validation of the High-Resolution Salish Sea Tidal Hydrodynamic Model*. PNNL-30448, 108pp.

Yang, Z., Wang, T., Branch, R., Xiao, Z. and Deb, M., 2021. *Tidal stream energy resource characterization in the Salish Sea*. Renewable Energy, 172, pp.188-208.

10 ACKNOWLEDGEMENTS

No additional acknowledgements to report.

11 APPENDIX

The following figures are simulated vs. observed velocity comparisons for all nine surveys on August 20th, 2020.

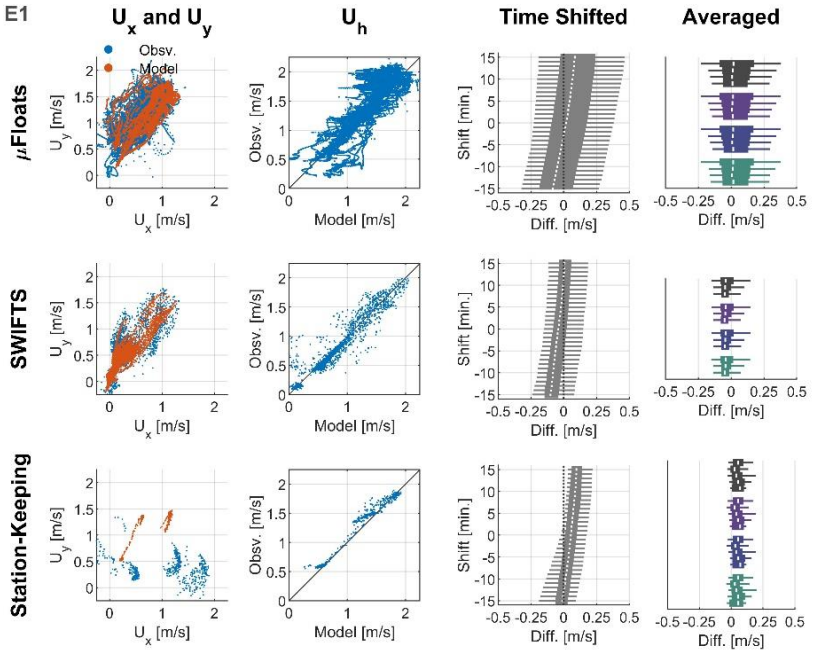

Figure A1a: Compiled comparison statistics for Survey E1

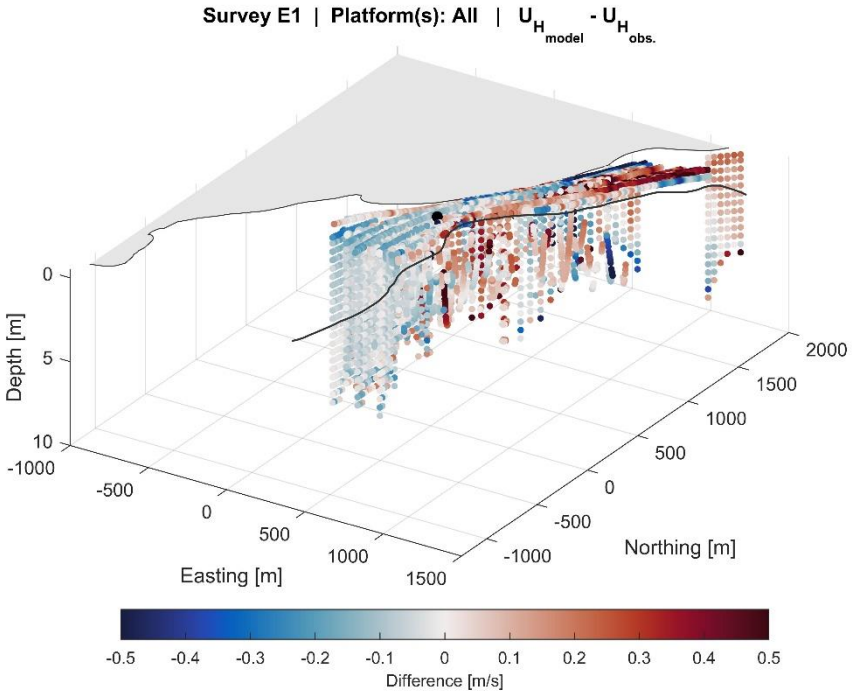

Figure A1b: Spatial distribution of simulation-observation differences for Survey E1

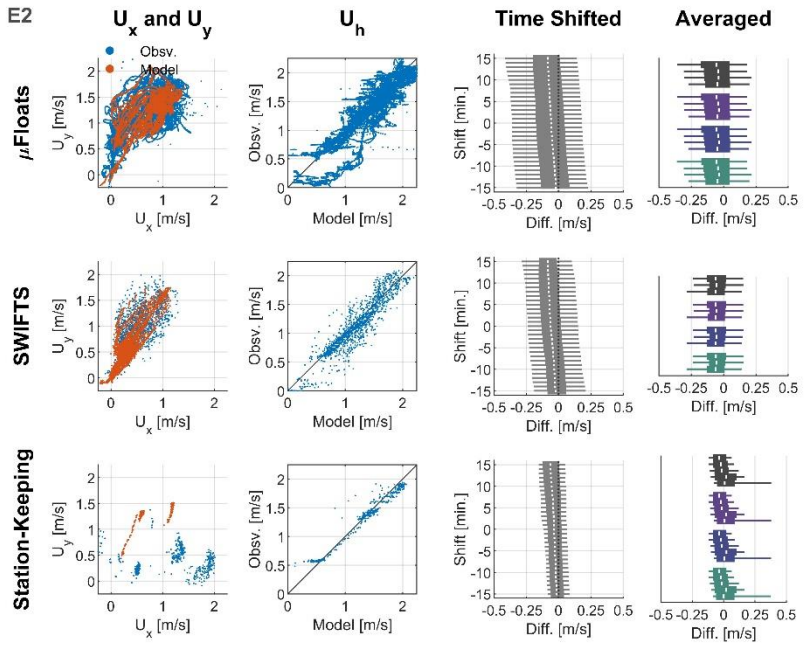

Figure A2a: Compiled comparison statistics for Survey E2

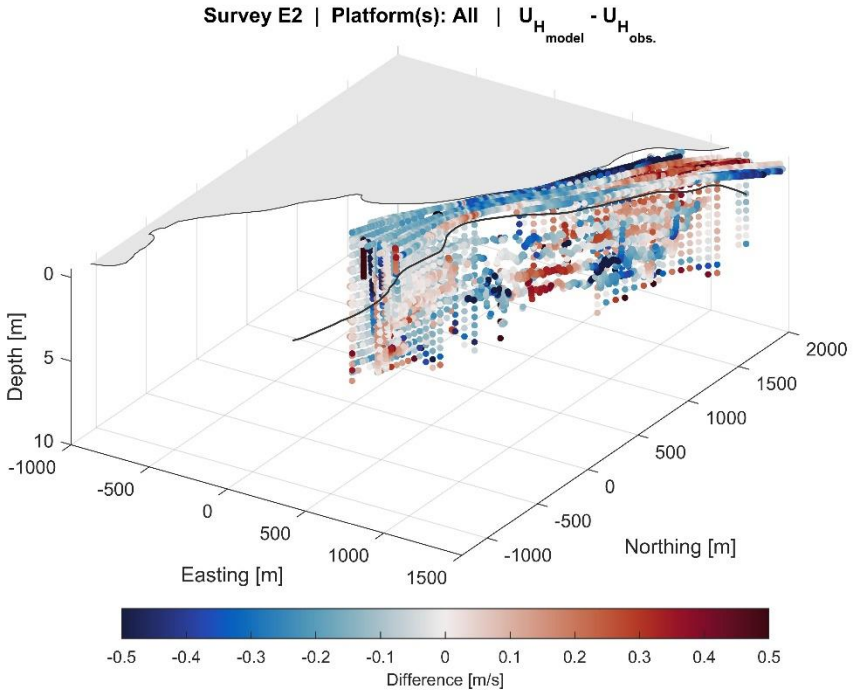

Figure A2b: Spatial distribution of simulation-observation differences for Survey E2

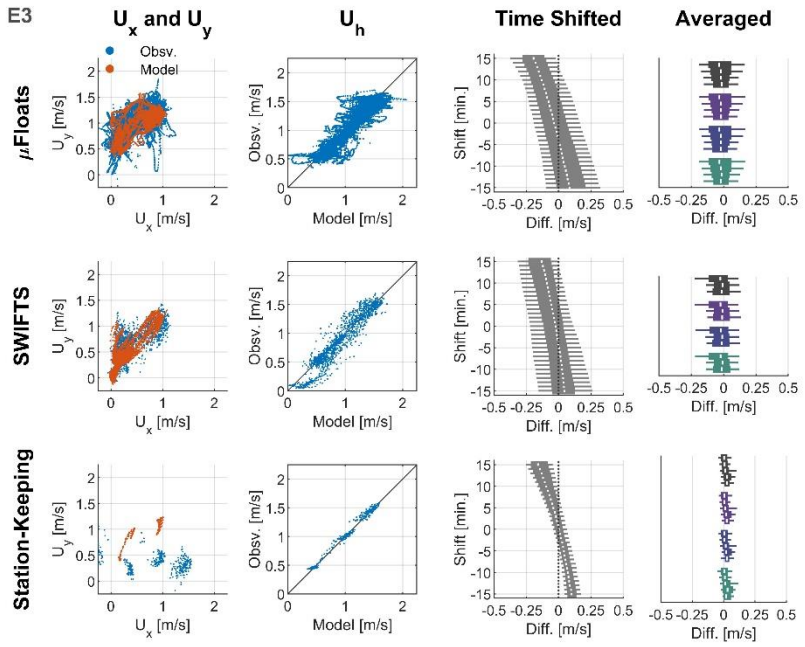

Figure A3a: Compiled comparison statistics for Survey E3

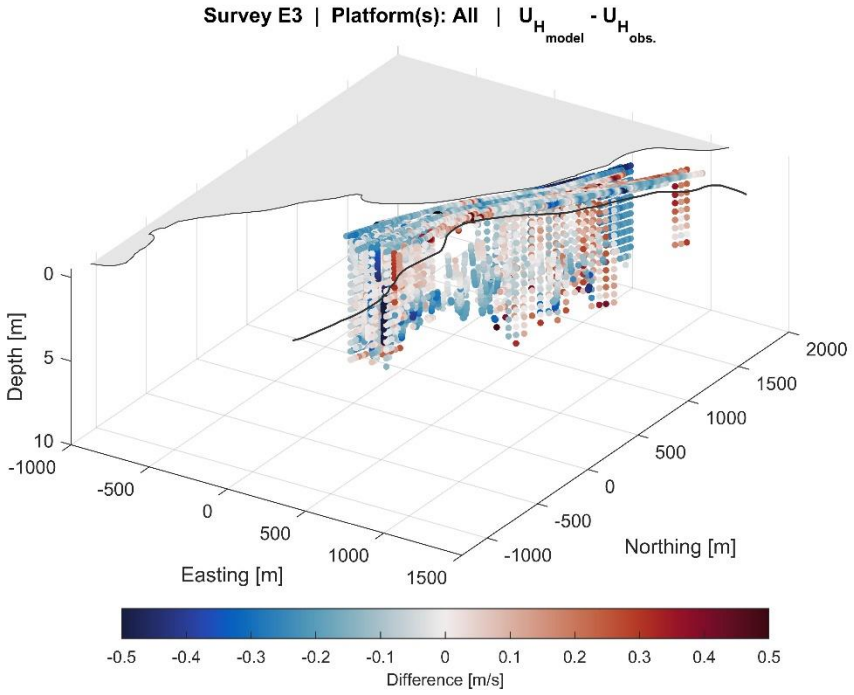

Figure A3b: Spatial distribution of simulation-observation differences for Survey E3

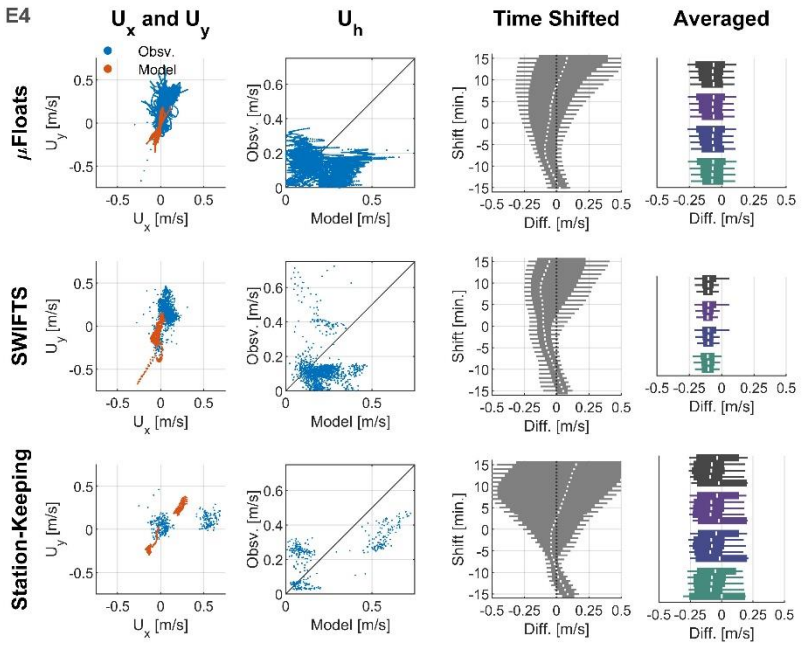

Figure A4a: Compiled comparison statistics for Survey E4

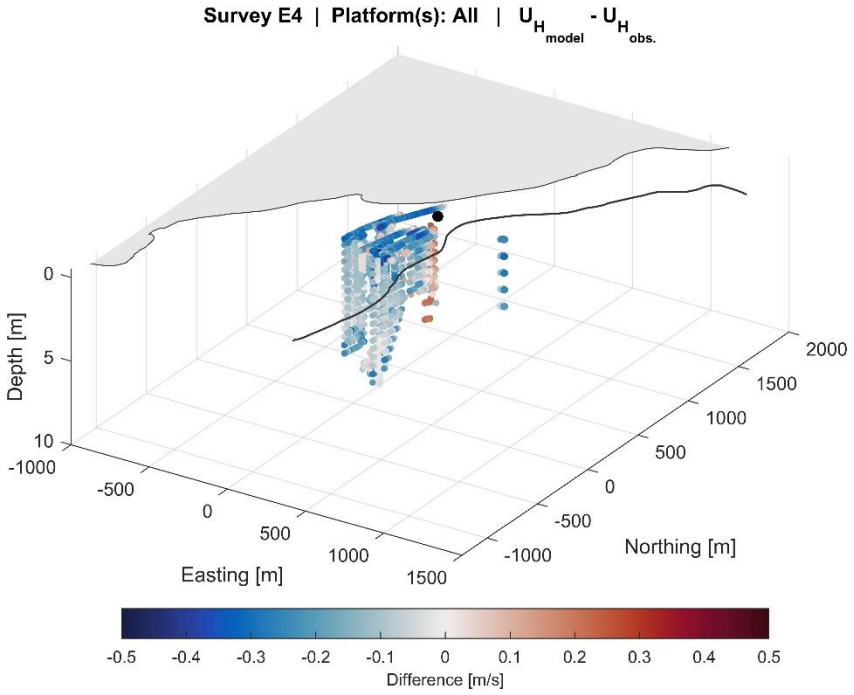

Figure A4b: Spatial distribution of simulation-observation differences for Survey E4

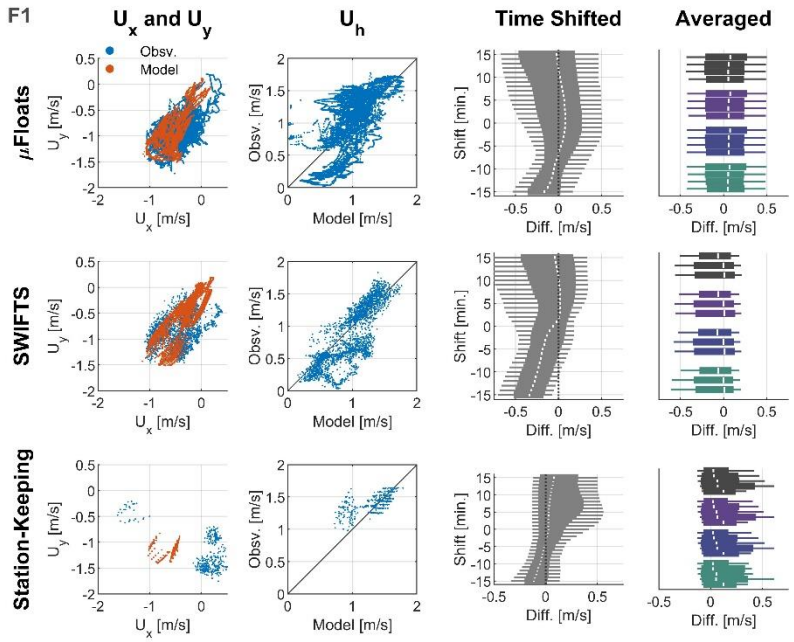

Figure A5a: Compiled comparison statistics for Survey E1

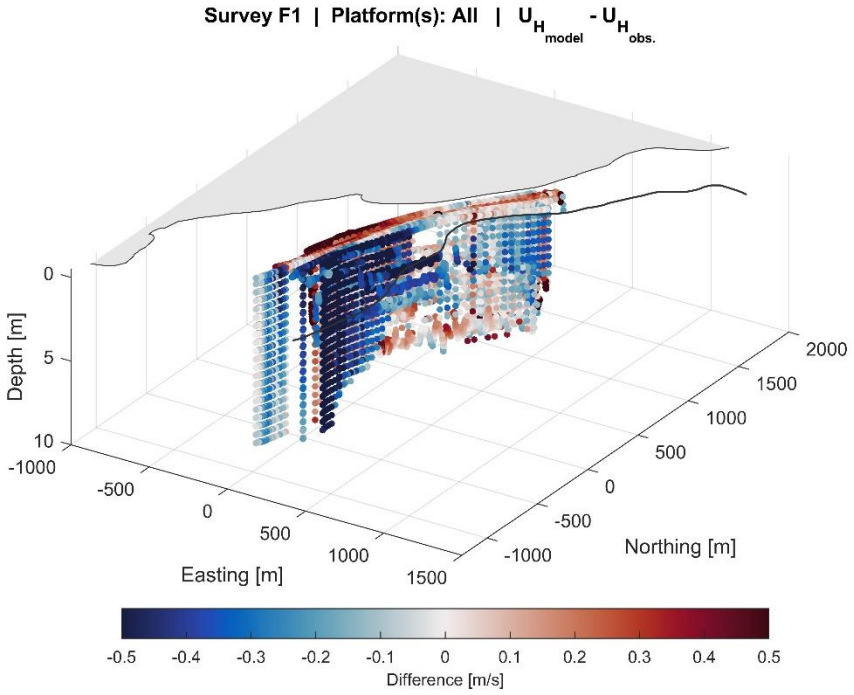

Figure A5b: Spatial distribution of simulation-observation differences for Survey F1

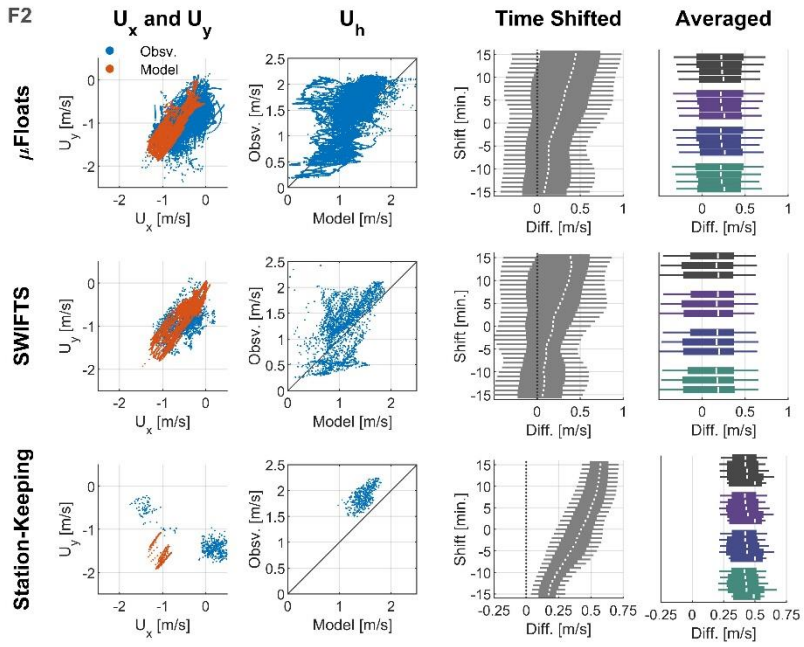

Figure A6a: Compiled comparison statistics for Survey F2

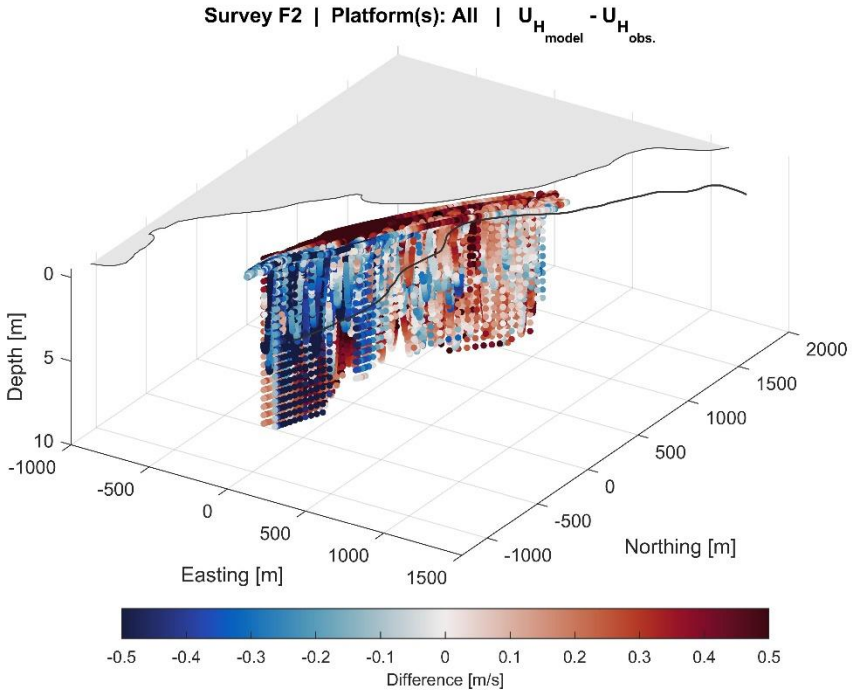

Figure A6b: Spatial distribution of simulation-observation differences for Survey F2

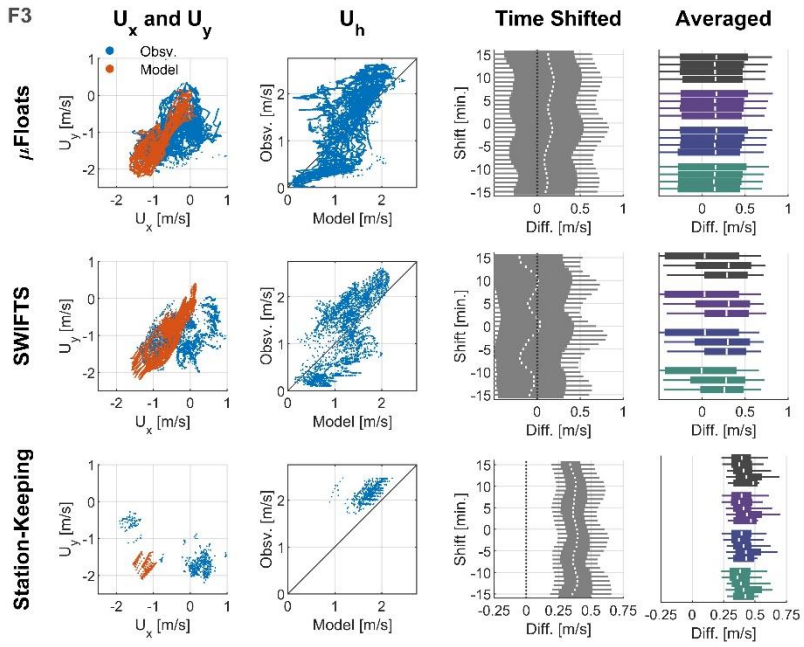

Figure A7a: Compiled comparison statistics for Survey F3

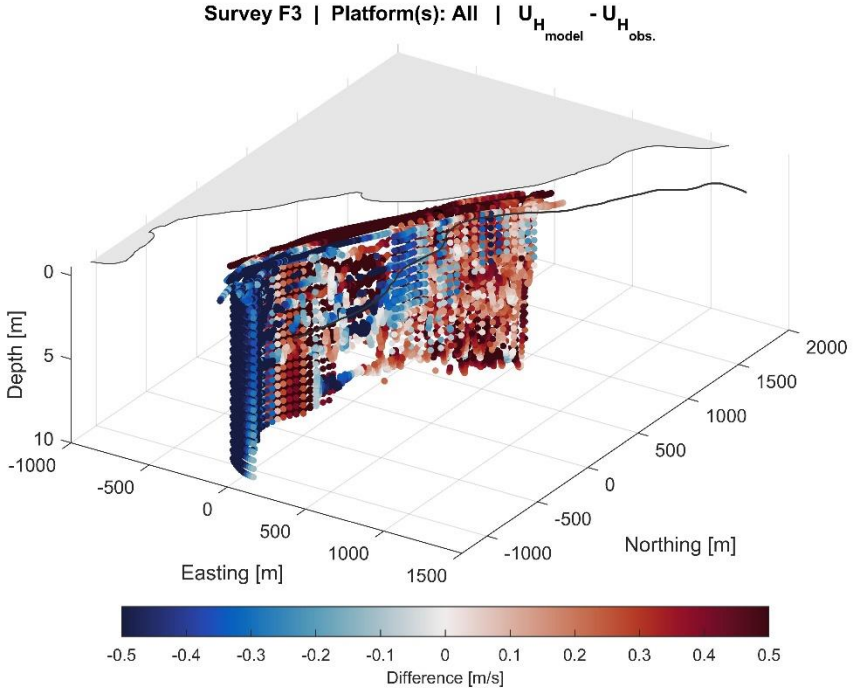

Figure A7b: Spatial distribution of simulation-observation differences for Survey F3

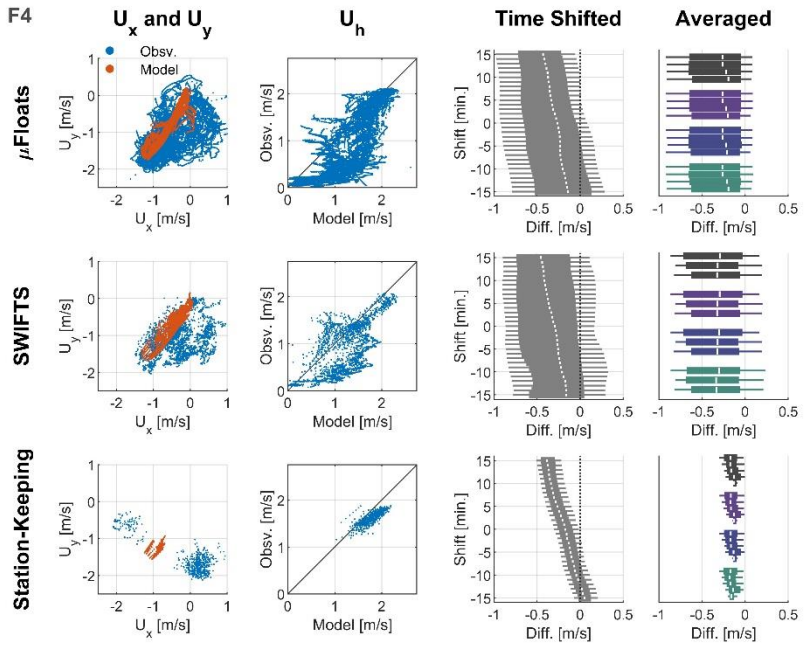

Figure A8a: Compiled comparison statistics for Survey F4

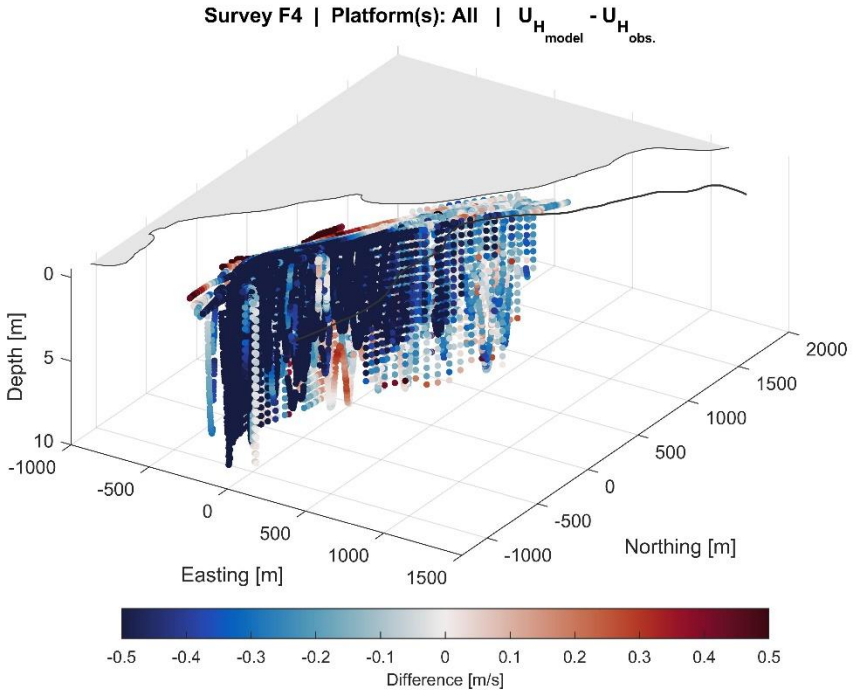

Figure A8b: Spatial distribution of simulation-observation differences for Survey F4

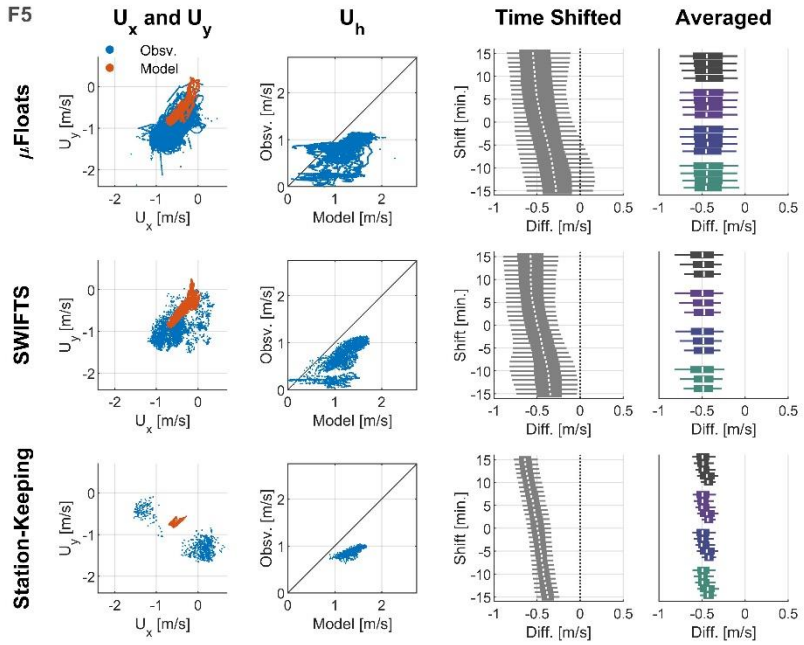

Figure A9a: Compiled comparison statistics for Survey F5

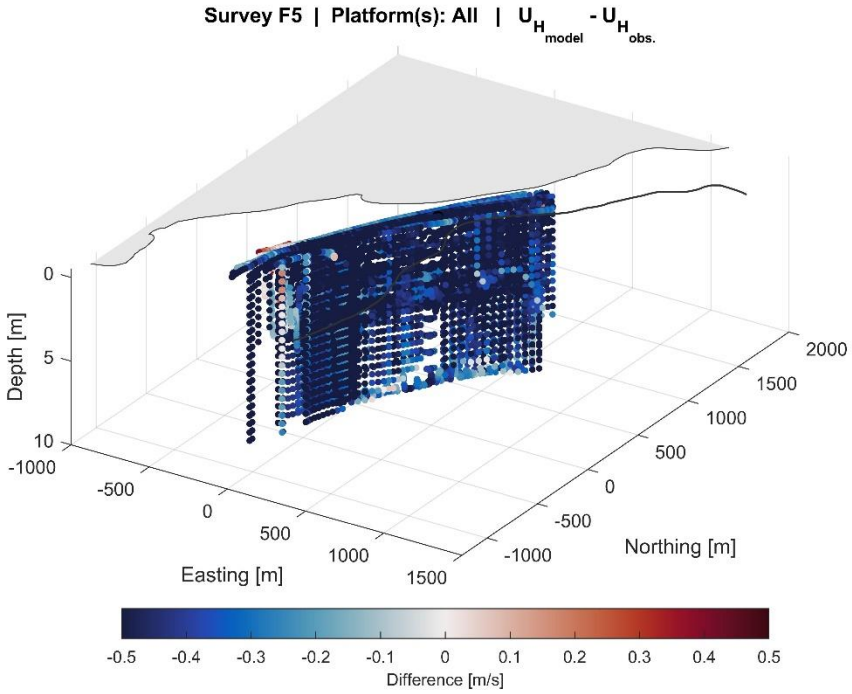

Figure A9b: Spatial distribution of simulation-observation differences for Survey F5